remote sensing

Review

Application of Remote Sensing in Detecting and Monitoring Water Stress in Forests

Thai Son Le [1,2], Richard Harper [1] and Bernard Dell [1,3,*]

[1] Agriculture and Forest Sciences, Murdoch University, Murdoch, WA 6150, Australia; thai.son.le@murdoch.edu.au (T.S.L.); r.harper@murdoch.edu.au (R.H.)
[2] Department of Environmental Management, Vietnam National University of Forestry, Hanoi 13417, Vietnam
[3] Forest Protection Research Centre, Vietnamese Academy of Forest Sciences, Hanoi 11910, Vietnam
* Correspondence: b.dell@murdoch.edu.au

Abstract: In the context of climate change, the occurrence of water stress in forest ecosystems, which are solely dependent on precipitation, has exhibited a rising trend, even among species that are typically regarded as drought-tolerant. Remote sensing techniques offer an efficient, comprehensive, and timely approach for monitoring forests at local and regional scales. These techniques also enable the development of diverse indicators of plant water status, which can play a critical role in evaluating forest water stress. This review aims to provide an overview of remote sensing applications for monitoring water stress in forests and reveal the potential of remote sensing and geographic information system applications in monitoring water stress for effective forest resource management. It examines the principles and significance of utilizing remote sensing technologies to detect forest stress caused by water deficit. In addition, by a quantitative assessment of remote sensing applications of studies in refereed publications, the review highlights the overall trends and the value of the widely used approach of utilizing visible and near-infrared reflectance data from satellite imagery, in conjunction with classical vegetation indices. Promising areas for future research include the utilization of more adaptable platforms and higher-resolution spectral data, the development of novel remote sensing indices with enhanced sensitivity to forest water stress, and the implementation of modelling techniques for early detection and prediction of stress.

Keywords: drought; forest management; leaf and canopy spectral traits; remote sensing platforms; vegetation indices; water deficit

check for updates

Citation: Le, T.S.; Harper, R.; Dell, B. Application of Remote Sensing in Detecting and Monitoring Water Stress in Forests. *Remote Sens.* **2023**, *15*, 3360. https://doi.org/10.3390/rs15133360

Academic Editors: Won-Ho Nam and Xiang Zhang

Received: 1 June 2023
Revised: 28 June 2023
Accepted: 29 June 2023
Published: 30 June 2023

1. Introduction

Climate change is increasingly impacting on the environment with obvious evidence [1–4]. Most noticeable is the increase in the average temperature globally that has led to changes in the Earth's hydrological cycle [5]. A global trend has been established that involves a widening of the tropical belt and a drying environment represented by an increase in both frequency and severity of adverse water-related phenomena, such as extreme droughts, temperature extremes, and heat waves [3,6,7].

Drought, a complex situation associated with low precipitation and low water availability in soils, is a significant driver shifting natural vegetation cover and promoting desertification with water stress leading to reduced growth and increased mortality in forest ecosystems [6,8,9]. Forest water stress is defined as the condition in which a forest experiences a prolonged or severe water deficit that exceeds the ability of the trees to cope with it, leading to physiological and ecological responses that can ultimately affect forest health and productivity. The symptoms of forest water stress can be broadly classified into two categories: physiological and ecological [10,11].

Physiological symptoms of forest water stress include changes in plant water status and gas exchange, as well as alterations in plant growth and metabolism. Water deficit disturbs physiological activities of plants that directly restrict their responses to the movement of other elements in the habitat. Lisar et al. [10] summarised the effects of water stress on plants as the alterations of photosynthesis, respiration, translocation, ion uptake, carbohydrates, nutrient metabolism, and hormones. Insufficient water availability initially decreases the water potential in plant cells and increases the concentration of dissolved substances in the cytosol and extracellular matrices [10–14]. The temporary consequences include growth inhibition and reproductive failure, and the accumulation of abscisic acid and compatible osmolytes (e.g., proline) that lead to wilting [12].

Through influencing plant water relations by reduction in leaf water content and turgor, water stress interrupts stomatal opening and closure, limits gaseous exchange, reduces transpiration and arrests photosynthesis [11,15]. These changes can lead to altered plant nutrient and hormonal balances. These responses are typically adaptive and can help trees conserve water and maintain basic physiological functions under water-limited conditions. However, interruption of water movement in the plant body brings mineral nutrient uptake and transportation and metabolism to a standstill, reducing cell expansion and organ enlargement due to low turgor pressure [16,17]. As a result, water deficit significantly decreases growth increments and overall plant performance [14,18,19]. The duration and intensity of stress [11] determine whether water deficit will cause dehydration, wilting, and mortality [20,21]. Mortality is the worst consequence of prolonged water stress in forests, and impact can vary from a few individual trees, scattered patches of trees (Figure 1), to collapse of large forest stands.

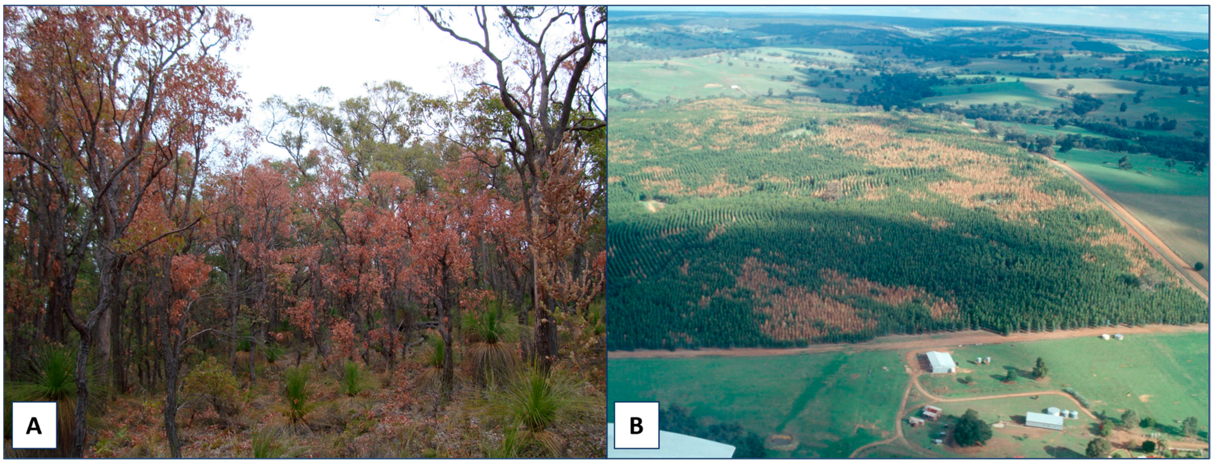

Figure 1. (**A**) Example of forest patch death resulting from water deficit in a dry sclerophyll eucalypt forest in Australia (photo B. Dell); (**B**) young *Eucalyptus globulus* pulpwood plantation affected by drought, alongside natural *Eucalyptus marginata* forest and cleared farmland, Western Australia, 1998 (photo R. Harper).

Ecological symptoms of forest water stress include changes in forest structure, composition, and function [22–25]. These changes can affect various ecosystem processes, including nutrient cycling, carbon sequestration, and water use efficiency [26,27]. For instance, water-stressed forests may exhibit decreased biomass production, increased mortality rates, and altered species composition. Moreover, changes in forest structure can affect microclimate conditions, soil properties, and understory vegetation, which can in turn affect biodiversity and ecosystem services. In addition, forest water stress can also increase the susceptibility of trees to biotic and abiotic stresses, such as insect attacks, disease outbreaks, forest fire, and extreme weather events. These secondary effects can exacerbate the impact of water stress on forest health and productivity [28–30].

In order to understand and to attempt to ameliorate the extent of tree decline, we need effective tools to detect and monitor water stress in forests. Recent remote sensing technology provides a number of advantages for Earth surface monitoring, including large coverage, diverse resolution, timely data collection, non-invasive and cost-effective acquisition [31,32]. Indeed, remote sensing imagery can provide valuable data from vegetation, soil, and environmental factors over large areas without physical contact [32–34]. This technology in association with a geographic information system (GIS) has widespread practical applications in the analysis of vegetation and environmental dynamics [31,35,36].

Remote sensing techniques are increasingly being used to measure forest water stress due to their advantages, especially in terms of spatial scale as compared with traditional ground-based methods [37–39]. These techniques, including satellite imagery, can provide information about water stress across large areas, even in remote or inaccessible areas, which can be particularly useful for monitoring forests at the regional or even global scale [40]. This is especially important given the significant role that forests play in the global water cycle and energy and carbon balances. Remote sensing techniques are non-destructive and can provide information about water stress without any physical contact with the forest [34,41]. Remote sensing technology can measure multiple indicators of water stress, such as water content, leaf pigments, canopy temperature and chlorophyll fluorescence, which can provide a more comprehensive picture of forest health and water use [33,39,42–44].

This review aims to provide an overview of remote sensing applications for monitoring water stress in forest and reveal the potential for remote sensing and geographic information system applications in monitoring water stress for effective forest resource management. It examines the principle and necessity of detecting plant water stress in forests using remote sensing technologies. From a quantitative literature review, we appraise a wide range of remote sensing applications in relation to plant water stress detection in forestry in order to identify overall trends. Lastly, we assess the potential of remote sensing and GIS applications in water stress monitoring for forest resource management.

2. Remote Sensing for Detection of Plant Water Stress

2.1. General Principles

The principle of remote sensing in vegetation observation involves using sensors to measure the different wavelengths of electromagnetic radiation emitted or reflected by plants and their surrounding environment [31,32]. Healthy vegetation reflects and absorbs different wavelengths in a characteristic way, which can be detected by remote sensing instruments [31,45]. For example, healthy vegetation absorbs most of the visible light spectrum, but reflects a high proportion of near-infrared radiation. This means that healthy vegetation appears green in visible composite images but appears bright in near-infrared images. By analyzing the patterns of reflected or emitted electromagnetic radiation, remote sensing instruments can provide information about vegetation properties such as leaf area index (LAI), chlorophyll content, water content, and biomass [46–49]. This information can be used to monitor vegetation health, identify areas of vegetation stress, and estimate crop yields [31,32].

This section provides a description of the remote sensing principles used to detect water stress in plants, mainly based on the imaging of signals at appropriate wavelengths. Figure 2 illustrates the spectral ranges of imaging methods that are available for monitoring plant response to water stress.

The typical spectral reflectance of vegetation exhibits high reflectance in the near-infrared (NIR) region (around 700–1300 nm) and lower reflectance in the visible region (around 400–700 nm) [50–52]. This is due to high chlorophyll absorption in the visible wavelengths and strong reflectance by the internal structures and water content of the plant cells in the NIR region [33,53]. Additionally, vegetation tends to have low reflectance in the shortwave infrared (SWIR) region (around 1300–2500 nm) due to the absorption by water and cellulose in plant tissues [37,54,55]. The interior leaf structure and biochemical components, such as greenness content (chlorophyll and carotenoid pigments), water, nitrogen, cellulose, and lignin, play a major role in the spectral characteristics of plants responding to radiation of different wavelengths [48,55,56]. The primary factors governing the spectral responses of leaves in the visible wavelengths are pigments, especially chlorophyll [45], which is closely related to photosynthetic capacity and overall primary productivity [45,57]. In addition, the cell structure of the leaf affects the spectral reflectance characteristics at NIR wavelengths, while the water content in the leaf governs the interaction with the wavelengths in the SWIR region.

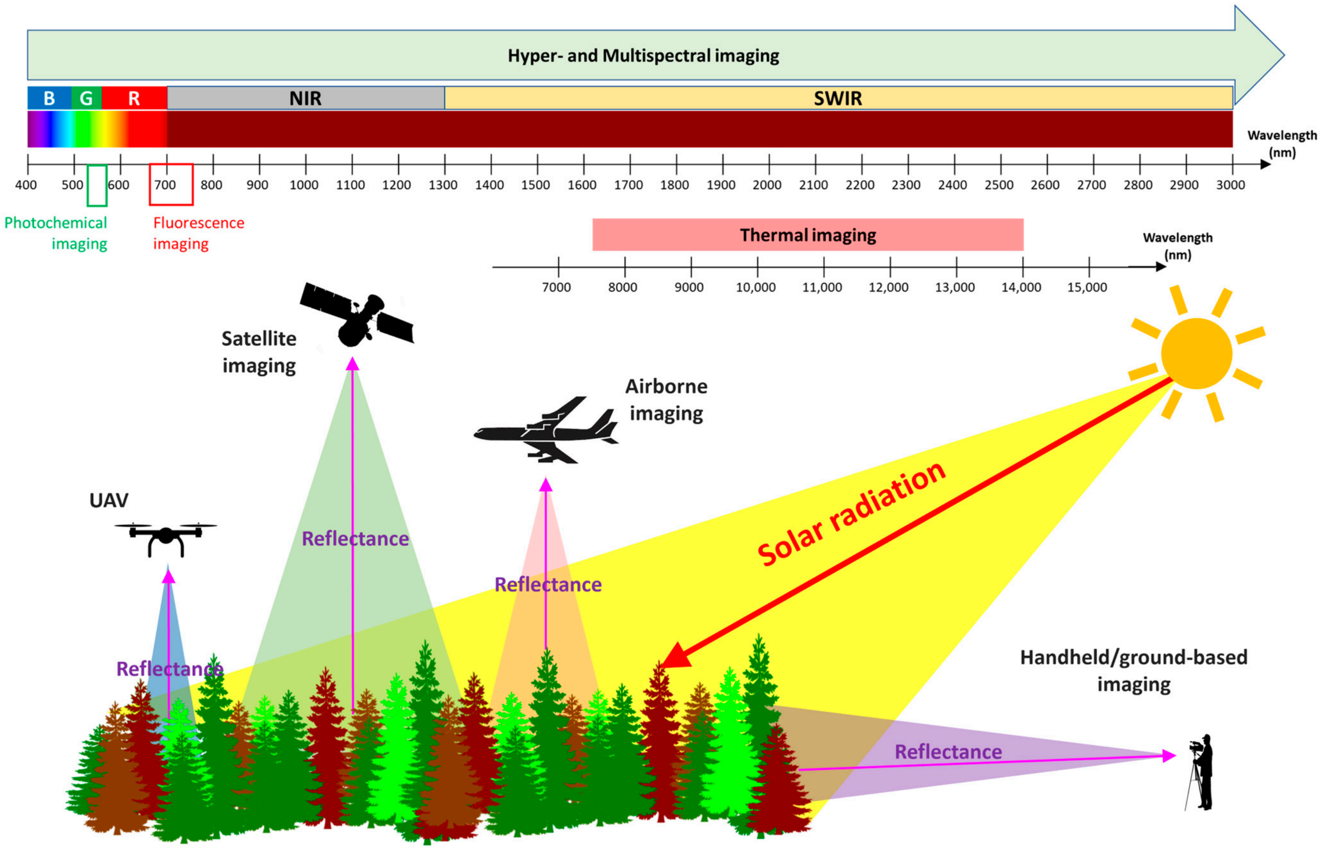

Figure 2. Main remote sensing platforms and imaging methods for detecting forest water stress (original by T.S. Le).

Water stress occurs when plants experience a shortage of water, leading to changes in their physiological and biochemical processes that reduce vegetation health [10,16,58]. These changes can be detected through remote sensing in order to monitor the health of plants and identify areas of water stress [32,40,59,60]. One way to detect water stress in plants is by measuring changes in the reflectance of visible and near-infrared light [40,59,61]. In general, stressed plants will have a lower reflectance in the near-infrared region and a higher reflectance in the visible region [45]. Another approach to detecting water stress is by measuring changes in the thermal properties of plants using thermal infrared sensors [39,44,62]. As plants become water-stressed, they may have a higher leaf temperature due to reduced transpiration for cooling and heat accumulation [10,63].

Numerous studies have confirmed the significant connections between leaf chlorophyll and water content, canopy temperature, and plant water stress [63–66]. Inferring that any reductions in greenness and water content are a sign of plant stress, these indicators, along with canopy temperature, have therefore been utilised as "surrogates" of plant water stress. There are several unique spectral bands and vegetation spectral reflectance indices that can be used to evaluate the chlorophyll and water content of plants [46,48,67]. With the rapid development of remote sensing in terms of spectral resolution, precision, and accuracy, measurements of narrower reflectance bands have allowed researchers to develop more innovative methods to detect plant water stress, including measurements of photochemical reflectance and chlorophyll fluorescence [68].

2.2. Vegetation Indices

A variety of vegetation indices (VIs) have been developed to monitor changes in vegetation and related physiological processes by utilizing the spectral reflectance characteristics of plants captured through different imaging methods combining reflectance at particular spectral wavelengths. Many of these indices, summarised in Table 1, have been utilised to detect water stress in plants. These include Typical VIs, Water VIs, Pigment VIs, and Temperature VIs. More detailed information concerning these indices and the principles and methods used to calculate them are provided in the corresponding references.

Table 1. Remote sensing indices that have been used for detecting plant water stress.

Vegetation Index	Formula	Reference
	Typical Vegetation Indices	
Simple Ratio Index (SR)	$SR = \frac{\rho_{NIR}}{\rho_{RED}}$	[69]
Normalised Difference Vegetation Index (NDVI)	$NDVI = \frac{\rho_{NIR}-\rho_{RED}}{\rho_{NIR}+\rho_{RED}}$	[52]
Soil-adjusted Vegetation Index (SAVI)	$SAVI = \frac{(\rho_{NIR}-\rho_{RED})(1+L)}{\rho_{NIR}+\rho_{RED}+L}$	[70]
Enhanced Vegetation Index (EVI)	$EVI = 2.5\frac{\rho_{NIR}-]\rho_{RED}}{\rho_{NIR}+C_1\rho_{RED}-C_2\rho_{BLUE}+L}$	[71]
Dynamic Relative Greenness Index (DRGI)	$\mathrm{DRGI} = \frac{ND_0-ND_{min}}{ND_{max}+ND_{min}} \times 100$	[72]
Perpendicular Drought Index (PDI)	$PDI = \frac{1}{\sqrt{M^2+1}}\rho_{RED} + M \times \rho_{NIR})$	[73]
Modified Perpendicular Drought Index (MPDI)	$MPDI = \frac{1}{\sqrt{M^2+1}}(\rho_{s,RED} + M \times \rho_{s,NIR})$	[74]
	Water Vegetation Indices	
Leaf Water Content Index (LWCI)	$LWCI = \frac{-\log(1-\rho_{NIR}+\rho_{SWIR})}{-\log(1-\rho_{NIR,FT}+\rho_{SWIR,FT})}$	[75]
Normalised Difference Water Index (NDWI)	$NDWI = \frac{\rho_{NIR}-\rho_{SWIR}}{\rho_{NIR}+\rho_{SWIR}}$	[76]
Moisture Stress Index (MSI)	$MSI = \frac{\rho_{1667}}{\rho_{927}}$	[46]
Shortwave Infrared Water Stress Index (SIWSI)	$\mathrm{SIWSI} = \rho_{SWIR} - \rho_{SWIR}\rho_{NIR} + \rho_{NIR}$	[77]
Vegetation Dryness Index (VDI)	$\mathrm{VDI} = 1 - \frac{A\prime E}{A\prime C\prime}$	[78]
Normalised Moisture Index (NMI)	$\mathrm{NMI} = \frac{\rho_{NIR}-\rho_{RED}}{\rho_{NIR}+\rho_{RED}} + \frac{\rho_{NIR}-\rho_{SWIR}}{\rho_{NIR}+\rho_{SWIR}}$	[79]
	Pigment Vegetation Indices	
Photochemical Reflectance Index (PRI)	$PRI = \frac{\rho_{531}-\rho_{570}}{\rho_{531}+\rho_{570}}$	[80]
”Green” NDVI	$GreenNDVI = \frac{\rho_{NIR}-\rho_{GREEN}}{\rho_{NIR}+\rho_{GREEN}}$	[81]
Normalised Difference Red-Edge index (NDRE)	$NDVI = \frac{\rho_{NIR}-\rho_{RED-Edge}}{\rho_{NIR}+\rho_{RED-Edge}}$	[82]
Chlorophyll Index (CI)	$CI = \frac{\rho_{NIR}}{\rho_{RED-Edge}} - 1$	[83]
Modified Photochemical Reflectance Index ($\mathrm{PRI_m}$)	$PRI = \frac{\rho_m-\rho_{570}}{\rho_m+\rho_{570}}$ m = 531, 515, 525, 535, 545 nm	[84,85]
	$PRI = \frac{\rho_{531}-\rho_m}{\rho_{531}+\rho_m}$ m = 512, 515, 551, 555, 602, 645, 667, 668 nm	[86]
	Temperature Vegetation Indices	

Table 1. *Cont.*

Vegetation Index	Formula	Reference
Crop Water Stress Index (CWSI)	$CWSI = \frac{(T_c - T_a)_m - (T_c - T_a)_{LL}}{(T_c - T_a)_{UL} + (T_c - T_a)_{LL}}$	[87]
Water Deficit Index (WDI)	$WDI = \frac{(T_s - T_a)_m - (T_s - T_a)_r}{(T_s - T_a)_m + (T_s - T_a)_x}$	[88]
Vegetation Water Supply Index (VWSI)	$VWSI = \frac{NDVI}{LST}$	[89]
Vegetation Temperature Condition Index (VTCI)	$VTCI = \frac{LST_{max}(NDVI_i) - LST(NDVI_i)}{LST_{max}(NDVI_i) - LST_{min}(NDVI_i)}$	[90]
Temperature Vegetation Dryness Index (TVDI)	$NDWI = \frac{LST - LST_{min}}{a + bNDVI - LST_{min}}$	[91]
Vegetation Water Temperature Condition Index (VWTCI)	$VWTCI = \frac{LST_{max}(VDI_i) - LST(VDI_i)}{LST_{max}(VDI_i) - LST_{min}(VDI_i)}$	[92]
Modified Vegetation Water Supply Index (VWSI)	$MVWSI = \frac{RNDVI}{RLST^2}$	[93]
Temperature Vegetation Soil Moisture Dryness Index (TVMDI)	$\sqrt{LST^2 + SM^2 + \left(\frac{\sqrt{3}}{3} - PVI\right)^2}$	[94]
Temperature Vegetation Water Stress Index (TVWSI)	$TVWSI = \frac{d(SWCI,\ NDVI)}{RLST}$	[38]

Typical VIs (Table 1) are calculated on the basis of the reflectance in the red (600–700 nm) and part of the NIR (700–900 nm) spectral regions, whereas Water VIs use reflectance in the SWIR bands. In addition, Pigment VIs reflect the concentrations of leaf pigments, mainly chlorophyll, by using green and red-edge reflectance. The red-edge narrow band around 700 nm is unique due to its correspondence to the threshold between the spectral regions with high light absorption (<700 nm) and high light reflectance (>700 nm) by chlorophyll pigments [95]. On the other hand, Temperature VIs have been developed with the participation of thermal infrared signals which provide information concerning land surface and canopy temperature. This information is usually combined with fractional vegetation coverage and Typical VIs to form a high-potential trapezoid theory to express the decline in plant physiological processes as a symptom of stress [91].

2.3. Spectral Characteristics of Leaf Chlorophyll Content

Chlorophyll is a pigment that plays a crucial role in photosynthesis, by which plants convert light energy into chemical energy. Specifically, chlorophyll molecules within chloroplasts in plant cells absorb light energy and use it to drive the synthesis of organic compounds such as glucose, which the plant uses for growth and metabolism. Chlorophyll is also responsible for giving plants their green colour, as it absorbs light most efficiently in the blue and red bands of the visible light spectrum and reflects green light.

Reduced leaf chlorophyll concentration in stressed plants alters the ability of plants to absorb solar radiation, changing their typical spectrum reflectance patterns by a decrease in green reflection and increases in red and blue reflections [83,96]. Therefore, remote-sensed detection of water stress in plant requires a determination of typical spectral reflectance patterns of healthy plants as a basis for comparison.

It has been established that certain reflectance wavelengths in the red and near-infrared spectrum are responsive to changes in chlorophyll pigments. Maximum reflectance sensitivity to chlorophyll contents have been reported at the wavelengths 550 and 700 nm (Figure 2) [51,68,97]. As a result, numerous spectral indices have been developed utilising the combination of spectral reflectance at these wavelengths by describing the relationships between the reflectance value and chlorophyll content of leaves, including the widely used normalised difference vegetation index (NDVI) [52] and various chlorophyll indices (CIs) [95,98,99]. However, these relationships are inconsistent because chlorophyll concentration can vary between plant species, with leaf age, or even among individuals of the same species in different habitat conditions. Coops et al. [48] recommend caution when using this type of index to estimate plant water stress across various plant species, crop types, or biomes.

2.4. Spectral Characteristics of Leaf Water Content

Water has a strong absorption feature in the mid-infrared (MIR) region (around 1300–2500 nm), and this absorption becomes more pronounced as the water content increases [100,101]. Therefore, plant tissues with higher water content tend to exhibit lower reflectance in the MIR wavelengths. Additionally, water content also affects the spectral reflectance in the visible and NIR regions. As water content decreases, the reflectance in the NIR region decreases while the reflectance in the visible region increases. Several studies have confirmed the significant correlation between NIR and MIR reflectance and water content in vegetation and soils [46,76,99–102].

Many water–vegetation indices have been derived from the reflectance of NIR, MIR, and SWIR regions of the electromagnetic spectrum. For assessing the water content in leaves utilizing remote sensing, Tucker [102] used a band within the range of 550 to 1750 nm. Furthermore, Musick and Pelletier [100] suggested using the ratio of spectral bands between 550–1750 nm and 2080–2350 nm. Nevertheless, in the laboratory study of Hunt and Rock [101], a strong correlation was observed between water content, leaf area, and the spectral index derived from the reflectance at 820 and 1600 nm. Especially in the SWIR region from 1400 to 2500 nm, strong relationships between specific spectral bands and many field measurements as indication of plant water stress, such as relative water content, leaf water potential, stomatal conductance, and cell wall elasticity, have been determined [46,54,103]. Faurtyot and Baret [54] also suggested that the spectral bands at 1530 and 1720 nm were optimal for assessing plant water content.

The normalised difference water index (NDWI) developed by Gao [76] is one of the most widely used indices for water content assessment as an indication of plant water stress. It is calculated using the NIR and SWIR wavelengths, which are sensitive to the presence of water in plant tissues. The formula for NDWI is $(\text{NIR} - \text{SWIR})/(\text{NIR} + \text{SWIR})$, where NIR refers to the reflectance at a near-infrared wavelength of 860 nm and SWIR refers to the reflectance at a short-wave infrared wavelength of 1240 nm. NDWI has been widely used to estimate water content for various tree species [104], particularly in areas where water availability is limited or where drought stress is prevalent [59].

2.5. Spectral Characteristics of Canopy Temperature

The spectral characteristics of canopy temperature refer to the way that plants emit thermal radiation in different parts of the electromagnetic spectrum, depending on their temperature [60,62,105]. The temperature of a plant canopy is influenced by a number of factors, including solar radiation, air temperature, humidity, and plant water use. In the thermal infrared (TIR) region of the spectrum, plants emit radiation at wavelengths between 800 and 1400 nm, which can be used to estimate their temperature [38,94,106].

When plants experience water stress, they close their stomata to reduce water loss, which in turn reduces evaporative cooling. This causes the temperature of the plant canopy to equilibrate with ambient conditions. In contrast, well-hydrated plants can maintain transpiration and evaporative cooling, resulting in cooler canopy temperatures [66]. Therefore, canopy temperature can be used as a direct indication of plant water stress. By measuring canopy temperature remotely using thermal infrared imaging, it is possible to detect water stress in crops and natural vegetation. The spectral characteristics of canopy temperature can be used to assess plant stress and water use efficiency [107], and to monitor environmental conditions such as drought, heat stress, and wildfire risk [32,39,108]. Various spectral indices have been developed using TIR data to estimate canopy temperature and detect plant stress, such as the crop water stress index (CWSI) [87] and the temperature vegetation dryness index (TVDI) [91].

The crop water stress index (CWSI) is a spectral index used to assess plant water stress based on vegetation temperature. It was developed to quantify the degree of water stress in crops, and it is calculated as the difference between the canopy temperature and the air temperature, normalised by the difference between the canopy temperature and the temperature of a well-watered reference surface.

TVDI is a spectral index used to assess vegetation water stress based on canopy temperature and the amount of vegetation cover. The TVDI is calculated by taking the difference between the surface temperature (measured by thermal sensors) and the temperature of the surrounding environment, and dividing it by the difference between the surface temperature and a reference temperature that represents maximum transpiration under the same atmospheric conditions. A higher TVDI value indicates more severe water stress, while a lower value indicates adequate water supply.

2.6. Spectral Characteristics of Plant Photosynthetic Efficiency

The photosynthetic efficiency of plants can be assessed using a variety of spectral characteristics. In addition to the common measure of chlorophyll content, the photochemical reflectance index (PRI) reflects changes in the xanthophyll-cycle pigment pool that protects the plant from excess light energys [80,85,99]. Additionally, the spectral response in the red and far-red wavelengths, including the emission of chlorophyll fluorescence, can also indicate changes in photosynthetic efficiency, as plants often adjust their photosynthetic machinery in response to changes in light conditions [65,108,109].

The PRI is a vegetation index that uses the difference in reflectance between the 531 and 570 nm wavelengths to estimate changes in the xanthophyll-cycle pigment pool [80]. PRI has been shown to be a sensitive indicator of plant stress, particularly in response to changes in light and water availability. PRI can be measured using high-resolution spectrometers or hyperspectral sensors that are capable of capturing narrow spectral bands in the visible and near-infrared regions. The PRI signal can be quantified using the PRI ratio, which is the difference between the reflectance at 531 and 570 nm divided by the sum of the reflectance at 531 and 570 nm. Zhang et al. [86] suggested using reflectance at other wavelengths (i.e., 512, 515, 551, 555, 602, 645, 667, 668 nm) instead of 570 nm. Gamon et al. [84] also developed PRI using alternative wavelengths (515, 525, 535, 545 nm) for 531 nm.

Chlorophyll fluorescence has distinct spectral characteristics that can be detected using remote sensing [65,68,110,111]. When plants absorb light energy in the photosynthetic process, some of it is dissipated as heat, while the rest is used to power the conversion of carbon dioxide and water into organic compounds. However, if the amount of absorbed light energy exceeds the amount needed for photosynthesis, excess energy is dissipated as fluorescence. Chlorophyll fluorescence emits in the red and far-red regions of the spectrum mainly in the 650–750 nm spectral range [112], with peak emission occurring at around 685 nm [68,113].

3. Remote Sensing Application for Water Stress Management in Forestry

Remote sensing applications for water stress detection and monitoring have developed rapidly since the 1970s, involving a wide range of techniques to examine water status in plants and damage from water deficit [33,114,115]. However, in spite of considerable investment in developing sensors and platforms as well as data processing, their applications have been mainly used to support irrigation in agricultural land where crops such as maize [47,105] and bean [104], are vulnerable to drought [33,116]. In the past, there has been relatively little research attention on remote-sensed methods to assess water stress in forests [23,36,41].

Increasingly, climate change is causing water stress in forests with significant adverse impacts on forest ecosystems, including changes in forest structure and composition, increased susceptibility to pests and diseases, and reduced carbon sequestration capacity [11,12,38,117]. Therefore, there is growing recognition of the importance of forest water stress as a critical issue for forest health and resilience, as well as for the provision of ecosystem services such as carbon sequestration, biodiversity conservation, and water regulation [5,23,32,38,39].

Interest in remote sensing applications for forest water stress management are gaining attraction as this could provide a more effective means of implementing forest management. Forest management practices, such as thinning, pruning, and selective harvesting, can help maintain soil moisture levels, reduce competition among trees for water, and promote efficient water use [117–119].

In the following sections, we provide a quantitative assessment of remote sensing applications in forest water stress management, utilizing Web of Science Core Collection (www.webofscience.com, accessed on 31 March 2023), CAB Abstracts (www.cabdirect.org, accessed on 31 March 2023), and Scopus (www.scopus.com, accessed on 31 March 2023). The search encompassed all publications indexed up until the date of access on 31 March 2023. The key words used for the search in the title, keywords, and abstract were "remote sensing" or "remotely sensed", "water stress" or "drought-stress", and in combination with "forest" or "forestry". The results were manually reviewed if an additional search detected the term "random forest". This is the name of an algorithm commonly used in remote sensing processing; however, it leads to confusion when attempting to locate studies related to forests and forestry.

3.1. Overall Trend of Remote Sensing Applications for Forest Water Stress Assessment

A total of 223 publications were found; 160 of them appeared in all searched databases. The total result is relatively small compared to the vast number of 1412 similar studies in agriculture (Figure 3).

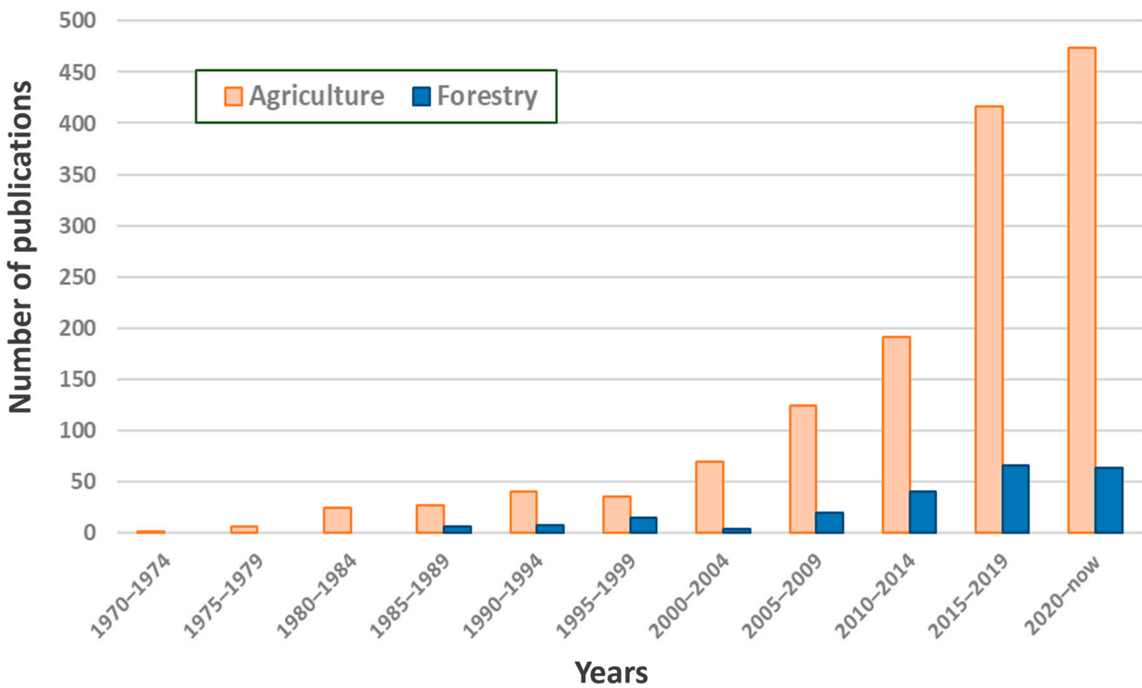

Figure 3. The number of publications on remote sensing applications for water stress assessment in forestry and agriculture by 5-year intervals (original by T.S. Le).

Of all the publications reviewed, the majority of works are concentrated in Europe and North America, as shown in Figure 4. This is understandable because these areas are where remote sensing technology was first developed and where numerous breakthroughs have occurred. However, there has been a significant rise in the number of publications from 2010 to the present for Asia, particularly in China. It is also worth noting that South America, which has the world's largest tropical rainforest ecosystem, has received recent interest due to the impact of climate change and an escalating risk of water stress. Overall, it is clear that many of the world's forests in the tropics and southern hemisphere are in need of further input into the remote sensing of forest condition.

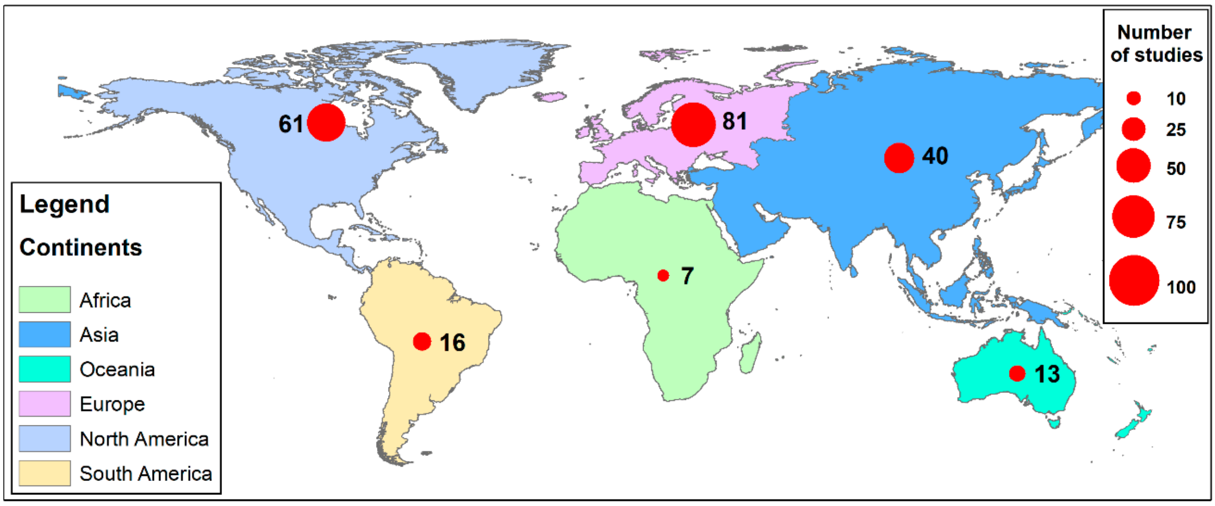

Figure 4. The number of publications on remote sensing applications for forest water stress assessment by region (original by T.S. Le).

Figure 5 shows the number of research subjects by forest type. The distribution of studies by geographical area in Figure 4 partly determines which forest types are the subjects of the reviewed studies. A significant proportion of the study areas are located in Europe and North America, which have temperate climates and are home to a diverse range of conifers and deciduous broadleaf species, such as *Quercus* (oak), *Fagus* (beech), and *Castanea* (chestnut). Research on evergreen broadleaf species is comparatively limited and primarily concentrated in the tropical forest areas of southwest China and the Amazonia rainforest. Additionally, there is an increasing trend in studying eucalypts in Australia, as some of these species, despite being considered drought-tolerant, are facing water availability limits in their natural habitats. In particular, advancements in satellite remote sensing technology have enabled studies to be conducted over vast territories that span multiple continents and encompass diverse forest ecosystems [120–123].

Satellite imagery has been preferred for water stress monitoring in forests (Figure 6). The main reason for this is that this imagery provides a wide coverage area, allowing for monitoring of large forested regions. This is especially beneficial for monitoring water stress in forests, which can occur at various scales, from individual trees to entire watersheds. Satellite imagery also provides timely and regular multispectral data that allow monitoring changes in water stress over time. Similarly, other parameters such as harvesting patterns or disturbances can be determined.

All digital information can be stored in databases, enabling users to study past phenomena and continuously monitor their evolution over extended periods. This long-term storage of satellite imagery data allows for historical analysis, facilitating the examination of past trends and changes in various environmental phenomena, including water stress in forests. By maintaining a historical archive of satellite imagery, researchers and forest managers can gain insights into the long-term dynamics of water stress in forests and track changes over time.

Regarding the types of spectral data used (Figure 7), the most preferred is reflectance in the visible and near-infrared bands. These bands are highly effective in capturing the distribution and condition of vegetation, primarily through widely used vegetation indices such as NDVI and EVI (enhanced vegetation index). Additionally, SWIR data are crucial as it can provide valuable information about the presence of liquid water in the forest canopy, which is directly related to water stress. Furthermore, thermal infrared data are increasingly being used, as it can detect abnormal increases in the temperature of water-stressed forest canopies caused by reduced cooling efficiency of plants through transpiration. There are a number of new applications based on the spectral space relations derived from the land surface temperature–vegetation index (LST-VI) combination [29,38,124,125].

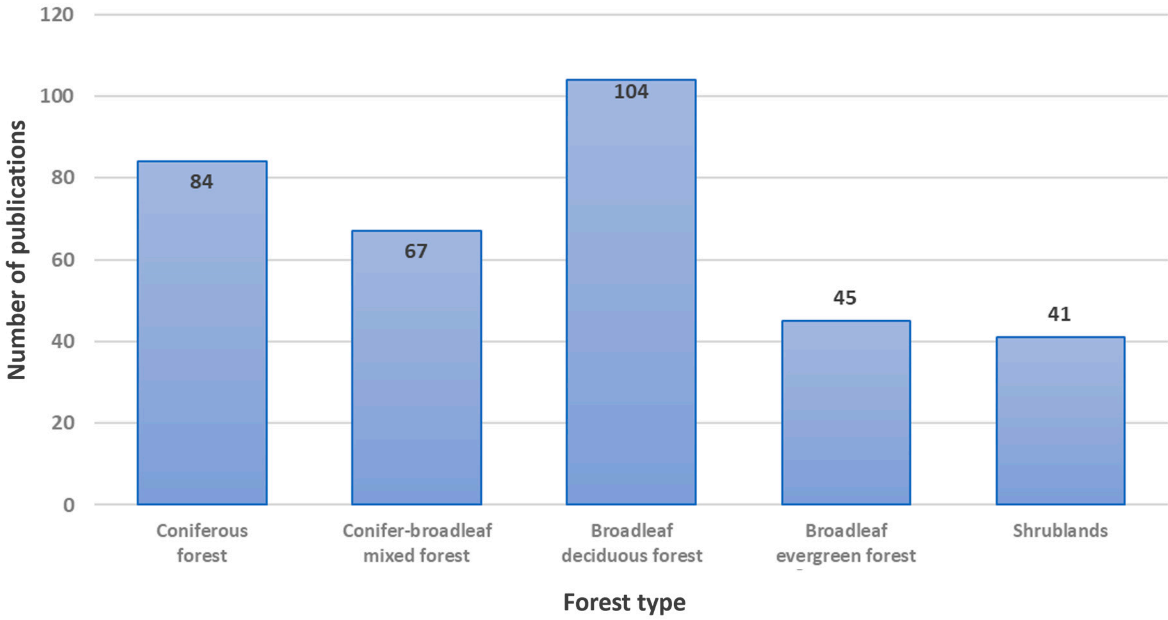

Figure 5. The number of publications on remote sensing applications for forest water stress management by forest type (original by T.S. Le).

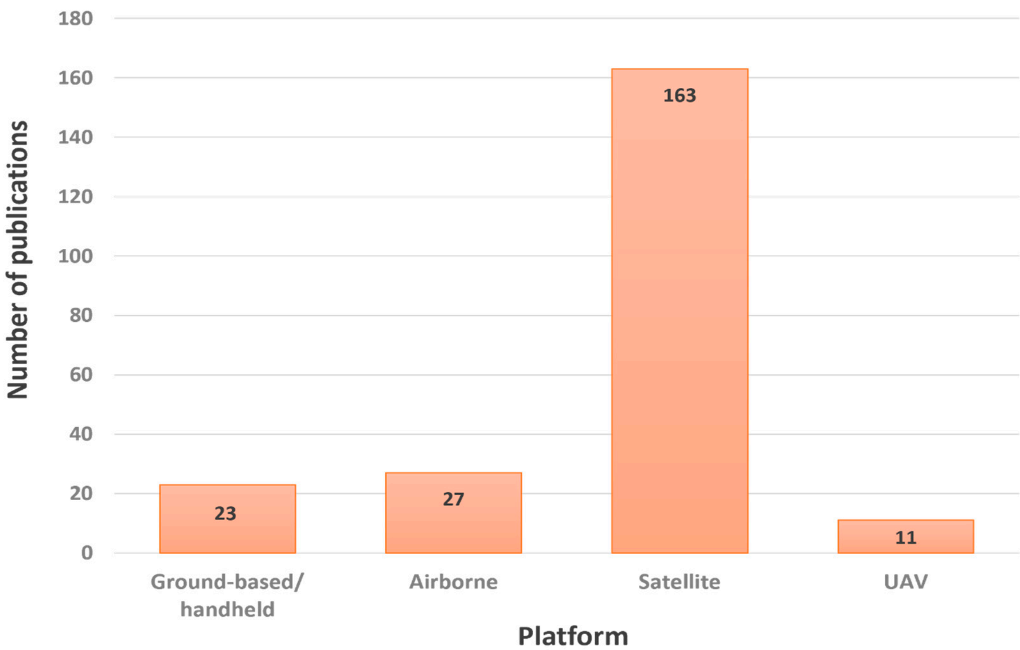

Figure 6. The number of remote sensing applications for forest water stress assessment by imagery platform (original by T.S. Le).

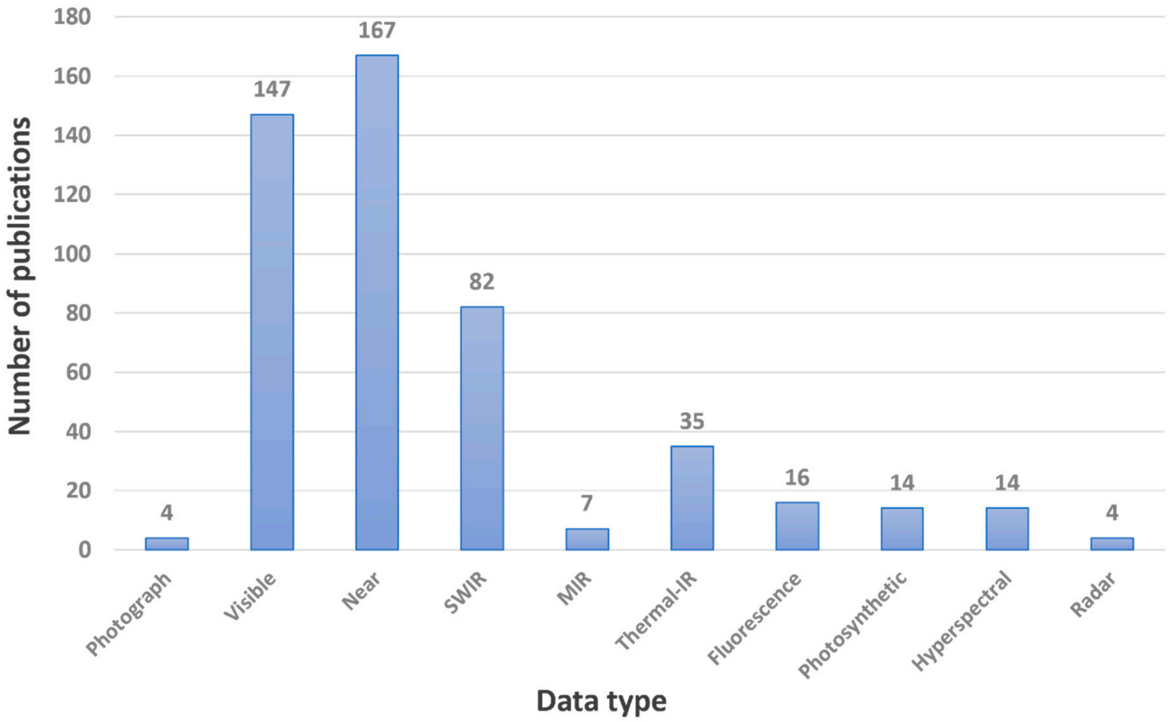

Figure 7. The number of applications on remote sensing applications for forest water stress assessment by data type (original by T.S. Le).

3.2. Change in Applications over Time

Earliest applications of remote sensing for forest water stress management appeared in the middle of the 1980s. These included studies by Korner [126] who used a thermal scanner to detect water stress symptoms in leaves, and Spencer [127] who applied large-scale 70 mm colour and black-and-white aerial photography to detect dieback in drought-stressed radiata pine. Spencer [127] emphasised the superior performance of colour photos as compared to black-and-white and field survey data. The use of satellite remote sensing to monitor forest–water interactions in water-limited sites was mentioned in the study by Running and Nemani [128], in which correlations between NDVI calculated from the Advanced Very High Resolution Radiometer (AVHRR) sensor and both photosynthesis (PSN) and transpiration (TRN) were examined. The result showed a correlation between weekly NDVI and PSN of up to $R^2 = 0.64$ on sites with substantial seasonal water stress. Correlations of weekly NDVI with TRN followed the same pattern as PSN, but they were slightly lower.

The effectiveness of aircraft-based remote sensing at the landscape scale was confirmed by Pierce et al. [129] for early-morning water stress detection in conifer forests in Germany using a wide range of bands. However, this study, in line with Hunt and Rock [101] and Cohen [130], stated that spectral reflectance from satellite imagery was not good enough to accurately detect water stress in forests, despite the established correlation between reflectance and water stress in plants [101,129]. Riggs and Running [131] also saw that water stress in conifer canopies might not be routinely detectable at an operational landscape scale due to the requirement of extensive ground data at times of aircraft operation.

However, Kalluri and Doraiswamy [132] advanced the field of research by calculating CWSI using a combination of Landsat and ground-based data in four separate districts in Iowa, USA. It was possible to determine the frequency, severity, and length of water stress using the temporal patterns of CWSI. The advantage of this technique was the possibility of application over large areas. This approach was supported by Vidal and Devauxros [133] with the Landsat-derived water deficit index (WDI).

Numerous new methods and applications of remote sensing techniques were introduced in the 1990s due to the outstanding development of many scientific disciplines and technologies, especially new sensors, and spectrometers with the capability to capture spectral reflectance in narrower bands. In the middle of the 1990s, a new technique was introduced by Gunther et al. [134] and Valentini et al. [135]. This involved the assessment of water stress by airborne laser-induced fluorescence of *Quercus pubescens* differentiating the ratio F685/F730 as a signal of stressed plants versus non-stressed plants. The effectiveness of this technique has been confirmed by many studies; however, it is still limited at a spatial scale to small clusters of trees and may only be applicable for ground-truth control measurements [134–137].

With the development of satellite imagery, there was a major trend in the late 1990s toward using AVHRR data to calculate vegetation indices (i.e., NDVI, LAI, WDI, and CWSI) as indicators of water stress [138–141], in which NDVI was the most popular index for applications, appearing in 75% of publications. In this period, vegetation water stress assessments preferred using simultaneous reflectance in the VIS, NIR, and TIR wavelengths, as available with the NOAA-AVHRR sensor [142] due to the advantages of its high temporal resolution (four images per day captured by two satellites) and multispectral bands (VIS, NIR, MIR, and TIR). The first use of PRI was in 1997 for stress detection in evergreen Mediterranean trees, including *Quercus ilex* and *Phillyrea latifolia*, [143] along with the introduction of the water index (WI) [144]. This opened a new direction in detecting stresses in plants in general.

The first decade of the 21st century presented breakthrough technology in spaceborne hyperspectral imagery with the launch of the Earth Observing-1 (EO-1) satellite in 2000, this carrying the Hyperion sensor. Spectroscopic data from this source were utilised to examine the dynamics of tropical rainforests and successfully detect drought stress in tropical forests, as well as monitoring forest physiology and carbon sequestration [145]. Although the Airborne Visible/Infrared Imaging Spectrometer (AVIRIS), another source of high-quality hyperspectral images of the Earth surface, had its debut in 1993, this imagery was unable to be applied to water stress monitoring due to low temporal resolution and costly expense [146].

In 2003, Europe experienced one of its warmest and driest summers, a precursor to future events affecting forest health due to climate change [147]. This event was a good opportunity for researchers to examine the condition and effects of drought stress and to develop new methods to assess, monitor, and predict similar events. Gobron et al. [147] assessed water stress areas over large areas of Eastern Europe using data from the Sea-viewing Wide Field-of-view Sensor (SeaWiFS) in association with the Medium Resolution Imaging Spectrometer (MERIS) sensor attached to the ENVISAT platform of the European Space Agency. Comparison with healthy vegetation in the year 2004 revealed the dramatic impact of the extreme drought on a variety of forest cover. Many other forest water stress studies have since been undertaken elsewhere in Europe using remotely sensed data from both spaceborne and airborne sources [72,148–151].

In addition to general vegetation indices such as NDVI, a wide range of new vegetation indices for water content assessment, such as NDWI [80], have been developed and validated for further applications in terms of forestry [152]. In the late 2000s, NDWI was one of the most preferred spectral indices for water stress monitoring in not only forestry but also in agriculture [153–155].

Eitel et al. [59] analysed the relationships between the actual water measurements of *Populus* spp. with NDWI, maximum difference water index (MDWI), the red-edge inflection point (REIP), and the water index (WI). The authors suggested that these indices exhibited significant relationships to high-severity water stress in poplar forests. However, the indices exhibited a lack of sensitivity in detecting low and moderate water stress levels in poplar in spite of the success in using SWIR-incorporating indices to detect water stress in other species. In another study, Jiang et al. [155] suggested using the shortwave infrared water stress index (SIWSI) with MODIS data instead of NDWI. Further study by

Jang et al. [79] integrated NDVI and NDWI to develop the new normalised moisture index (NMI). This study also presented a negative correlation between NMI and canopy surface temperature as an indicator of water stress. Satellite-based PRI was first used in forestry when Goerner et al. [156] tracked seasonal drought effects on a Mediterranean *Quercus ilex* forest using MODIS data. For this forest type, the drought-induced reduction in gross primary productivity estimated by PRI achieved higher accuracy as compared with the traditional MODIS-GPP algorithm [156]. This was supported by two other studies [157,158].

During the 2010s, there was a notable advancement in all methods employed for monitoring forest water stress. This progress was characterised by an expanded applicability to various forest types and the integration of existing remote sensing indices to create novel ones that exhibited enhanced sensitivity to stress conditions. For example, Ishimura et al. [159] used the improved temperature vegetation dryness index (iTVDI) to observe Japanese beech forest decline caused by air pollution and water deficits, and established that the improved index could detect tree collapses more accurately than the traditional NDVI and the former TVDI. The most popular applications involved mapping water stress by calculating basic vegetation indices, such as NDVI and EVI, from satellite-based data, especially MODIS and Landsat [40,160–162].

With the operation of the Greenhouse Gases Observing Satellite (GOSAT) in 2009, which provides sun-induced chlorophyll fluorescence data, the physiological and biochemical processes of forest trees can be evaluated from space instead of using handheld fluorometers. Lee et al. [163] used these data to model forest productivity under the impacts of water stress in Amazonia evergreen forests. They found that the variance in observed monthly mid-day fluorescence from GOSAT was a consequence of water stress.

The rapid development of unmanned aerial vehicles (UAV) and recognition of their potential resulted from upgraded battery duration for longer flight. As a result, many studies have explored using this platform with an appropriate sensor to measure water stress in forests [164–167]. For example, Gomez-Candon et al. [168] used UAV remotely sensed thermal images in combination with VIS and NIR data to assess water stress at the tree scale. The findings demonstrated a strong correlation between calibrated thermal images and ground-truth data. In comparison to healthy trees, those under water stress had significantly higher canopy temperatures.

A new application of radar remote sensing was developed by Steele-Dunne et al. [169]. By examining scatterometer data captured from a cluster of trees, the authors indicated that the difference in C-band wind scatterometer measurements between descending and ascending passes of the European Remote Sensing (ERS) satellite corresponded to the onset of vegetation water stress. Following the same approach, Konings et al. [170] determined the water stress status in the humid tropical forests of Central Africa at basin scale using radar backscatter from QuikSCAT (2001–2009) and RapidScat (2014–2016) at 0.25° grid-cell resolution. The findings revealed that diurnal variations in RapidScat backscatter effectively showcased the occurrence of widespread mid-day stomatal closure in the studied forests. The results clearly indicate that microwave and radar technology hold significant potential for monitoring water stress in forests. Notably, active remote sensing systems, which have already been proven effective in agricultural drought monitoring, were extensively reviewed by Vreugdenhil et al. [171]. The advancements and challenges associated with these technologies in the agricultural sector highlight their promising prospects for similar applications in forestry. However, it is worth mentioning that there are a limited number of published studies exploring their utilization in forest ecosystems. Nonetheless, the accomplishments witnessed in agriculture bolster the viability of employing these methods for water stress monitoring in forests in the near future.

Modelling the impacts of water stress on forest ecosystems was a new research direction restated during the decade. Sun et al. [172] tested the water supply stress index (WaSSI), a monthly water–carbon balance model, for potential application in addressing the influences of water stress on natural ecosystem services in the US. The authors suggested that the WaSSI model was successful in simulating long-term water–carbon balances in forests at a watershed scale. In the same year, Brouwers et al. [161] used Landsat data for water stress mapping in an evergreen eucalypt forest under a Mediterranean-type climate. This study also produced a damage probability model from a set of topography and climate-related factors in association with the probability of drought/heat stress within the forest. The application can be easily adapted to other regions to support forest management to mitigate water stress damage.

In the late 2010s, there was an increase in the number of applications monitoring water stress by the canopy water content (CWC) measurements from airborne imagery [173–175]. These studies measured CWC in conifer forests at landscape scale in association with leaf-level physiology measurements and crown-level foliage dieback surveys. The results proved that CWC or change in CWC were useful for water stress detection by revealing patterns of potential foliage damage and canopy collapse in conifers. However, the necessity for aircraft equipped with high-quality hyperspectral sensors presents a significant challenge for the widespread adoption of this method.

In recent years, determining the response of forest trees and ecosystems to water deficit, droughts, and heat waves, and changes in water–forest interactions, have been a focus of research as solutions to manage an increasingly warmer and drier environment are sought. In such studies, remote sensing techniques have been effective because of their applicability at landscape scale [29,176,177]. In addition, the 2018 drought event in Europe, which was climatically more severe and had more serious impacts on forest ecosystems than the 2003 drought, has raised more awareness by forest managers and researchers regarding forest water stress, and it also precipitated studies in regard to the response of forests to drought and the effects of water stress on large-scale forest health [178,179].

In addition, new spectral indices have been developed for forest water stress assessment based on indices previously applied to agricultural crops. Avetisyan [180] introduced the plant senescence reflectance index (PSRI2) comprising two red-edge bands (705 and 783 nm) and the green peak band (560 nm) from the Sentinel-2 satellite. This index was tested in broadleaf forests, coniferous and mixed forests, and transitional woodlands/shrubs, whereas the original PSRI was used for field crops and fruit trees [181]. Another study by Masiello et al. [182] utilised hyperspectral data from Infrared Atmospheric Sounder Interferometer (IASI) mounted on European Space Agency's MetOp satellites to develop the IASI water deficit index (IASI-WDI) to monitor water stress in Mediterranean forests in Italy. The study also produced a time series of the index that indicated the atmospheric background conditions associated with any meteorological drought causing stress in the forest. The most recent index is the temperature vegetation water stress index (TVWSI) developed by Joshi et al. [38], which comprises three indicators associated with plant water stress: canopy temperature through LST, canopy water content through the surface water content index (SWCI), and canopy fractional cover through NDVI.

A new application of remote sensing in monitoring water stress in urban forestry was provided by Fuentes et al. [183]. The study captured images by an integrated visible and infrared thermal camera to calculate effective leaf area index (LAIe) and the newly introduced tree water stress index (TWSI) derived from CWSI [87]. The relationships between TWSI and LAIs were mapped to highlight water-stressed tree locations among healthy urban green infrastructure. Furthermore, Ma et al. [110] monitored forest water stress using satellite solar-induced chlorophyll fluorescence (SIF) data, canopy fluorescence yield (SIFyield) data, and multisource remote sensing indices, including vegetation indices (NDVI, EVI), leaf area index (LAI), and fraction of absorbed photosynthetically active radiation (fPAR). Results from a performance analysis showed that SIFyield achieved a higher sensitivity to water stress, giving an earlier response to water deficit in forests than other indicators, and with an abnormal change higher by at least 10%. Recent studies also confirmed the potential of SIF in association with the standardised precipitation evapotranspiration index (SPEI) in forest water stress detection [177,184,185].

3.3. Overall Findings

Forest water stress management has been gaining greater interest in the context of climate change and increase in both frequency and severity of drought globally. With a rapidly growing number of publications each year, the most popular applications involve large-scale satellite-based data, especially reflectance at visible and infrared wavelengths, to observe water stress symptoms and damage to ecosystems, and to monitor the recovery of forests after stress. The use of UAV-based imagery and new types of remotely sensed data, such as satellite-based solar-induced chlorophyll fluorescence and hyperspectral images, is trending with the overall development of global science and technology. Furthermore, there is a continued need to enhance the analysis of canopy spectral reflectance using vegetation indices in order to effectively describe the water status in forests. The introduction of new indices with higher sensitivity in conjunction with higher-quality data as well as improvements and integration of existing indications are promising avenues for research.

Indeed, a wide range of VIs has been tried on forest water stress monitoring, as shown in Table 1. However, the wide distribution of water stresses across forested areas necessitates the use of remote sensing data with extensive coverage for effective analysis and monitoring. As a result, studies have primarily prioritised the use of satellite remote sensing data, which provides extensive coverage through broad image scenes. A significant limitation arises from the low resolution of these data, rendering it impossible to calculate vegetation indices with narrow wavebands, such as pigment vegetation indices. Similarly, water vegetation indices utilizing basic waveforms, such as NDWI or SIWSI, yield unsatisfactory results when applied to forest objects [154,186,187]. The current development of these indicators predominantly revolves around testing increasingly narrower wavelengths, which unfortunately are incompatible with satellite remote sensing data [80,85,86] at this time. Consequently, widespread usage remains concentrated on a few simple indices, notably NDVI and EVI [187–190]. Although these indices effectively assess damage to forest resources caused by water stress, they do not effectively facilitate early detection and continuous monitoring of water stress progression.

Recently, there has been a growing trend in employing temperature vegetation indices [191–193]. These indices derive their strength from the combined analysis of spectral reflectance, indicating the presence of vegetation stress even before visible damage occurs, and the variation in temperature conditions within the canopy. The temperature fluctuation serves as an indicator of the forest's cooling system efficiency, which diminishes in the absence of water [38]. This information is valuable for monitoring purposes. Notably, the application of temperature vegetation indices has produced significant and meaningful results. Looking ahead, the potential for temperature vegetation indices is poised to expand further, especially with the integration of thermal infrared sensors into UAVs. This advancement holds promise for enhancing the effectiveness of monitoring water stress in forests.

4. Integration of Remote Sensing of Water Stress with Other Spatial Datasets for Forest Management

Published studies have indicated that various environmental factors influence water stress in forests, including climatic conditions, soil and vegetation cover, hydrology, and topography [194–196]. Climate and weather features play a crucial role in the development of water stress in forests, as do features of the forests themselves, such as overall leaf area and the species involved.

Factors such as temperature, precipitation, humidity, and evapotranspiration can impact the overall water balance and thus availability of water in forests. With climate change, extended periods of high temperatures or drought can increase water stress in forests by reducing water availability and increasing water demand by vegetation.

Soil characteristics, such as soil texture, structure, and depth in particular, can also affect water stress in forests. Soil with low water holding capacity or poor drainage may limit the availability of water for plant uptake, leading to water stress. Soil properties also influence the rate of water infiltration, which can affect water availability for tree roots.

The type, density, and health of vegetation in forests can also influence water stress. Dense vegetation can compete for limited water resources, potentially leading to water stress in individual trees or stands. Additionally, the type of vegetation, such as species composition and physiological traits, can affect water-use efficiency and tolerance to drought. In addition, topographic variables, including slope, aspect, and elevation, have impacts on water stress in many ways.

Slope directly contributes to hydrological processes, such as runoff, groundwater recharge and discharge, and streamflow, which influence how water is spread within the ecosystem, and thus determine which areas have less water availability than others. In the northern hemisphere, south- or west-facing aspects may experience higher water stress due to increased solar radiation and evapotranspiration rates, while north-facing slopes may retain more moisture. Elevation can also affect temperature and precipitation patterns by forming microclimate conditions.

The strong development of GIS and computer science makes it easier than ever to represent those environmental factors in the form of spatial data sets. Simulation of environmental factors constituting forest water stress in a GIS is ideal for performing spatial analyses to consider the risk of this phenomenon occurring. Clearly, besides assessing water stress patterns and damage, forecasting the risk of this phenomenon is very important. Precise prediction and early detection are the basis for successful interventions to minimise damage to the ecosystems, which is the main goal that sustainable forest management aims at. Until now, there have been limited studies that have developed such forecasting models. Commonly used models are only general drought forecasting models that rely on meteorological models and water balance calculations at the watershed scale, without considering the response of vegetation or the distribution of different levels of stress in the ecosystem [197–200].

Different from agricultural crops, forests with water stress cannot be supported by irrigation and they depend solely on natural water sources, such as precipitation and soil water reserves. As climate change tends to reduce the amount of water input to natural ecosystems, interventions should aim at reducing water consumption by ecosystems. Ecological thinning and prescribed burning have been considered as the most feasible solutions which help reduce competition for water among trees and alleviate water stress in forests [117]. However, implementing such silvicultural interventions requires significant resources in terms of time and labour, making it challenging to carry out on a large scale across the entire forest. This underscores the importance of developing models that can predict and detect water stress early, allowing for proactive management actions to be taken in a targeted and efficient manner. The initial modelling results of Brouwers et al. [161] and Avetisyan et al. [201] are examples for this promising direction of research.

5. Conclusions

As global temperatures rise and precipitation decreases, the likelihood of water stress occurring in forest ecosystems is increasing. This review indicates that traditional methods for determining water stress are less applicable for large forest areas, which has led to the growing use of remote sensing technology, particularly satellite images, over the past two decades to overcome the issue of spatial scale. Nevertheless, traditional ground-based methods remain invaluable for validating the accuracy of remote-sensed measurements and for the validation and calibration of models derived from remote sensing. One of the most popular remote sensing applications is the use of visible and near-infrared spectrum bands in satellite remote sensing images, along with basic vegetation indicators, to monitor changes in vegetation and assess the effects of water stress. The advancement of remote sensing methods, utilizing more flexible platform and higher-resolution spectral data, has established the way for the emergence of new remote sensing indices that exhibit greater sensitivity to water stress. UAVs and data from solar-induced chlorophyll fluorescence and hyperspectral images hold promise for increased use in future applications. However, it remains challenging to replace the widespread use of popular satellite images like MODIS, Landsat, and Sentinel-2 due to their popularity, accessibility, and historical records. In the near future, it will be important to combine the results of studies on the response of forests to water stress with environmental factor datasets, to assess the likelihood of water stress occurring in forest ecosystems in the context of climate change. These applications are crucial for providing interventions to manage forest resources in a sustainable manner.

Author Contributions: Conceptualization, B.D. and R.H.; methodology, T.S.L. and B.D.; software, T.S.L.; writing—original draft preparation, T.S.L.; writing—review and editing, B.D. and R.H.; visualization, T.S.L.; supervision, B.D. and R.H. All authors have read and agreed to the published version of the manuscript.

Funding: There was no funding received for the study.

Conflicts of Interest: The authors declare no conflict of interest.

References

1. Trenberth, K.E.; Dai, A.; Van Der Schrier, G.; Jones, P.D.; Barichivich, J.; Briffa, K.R.; Sheffield, J. Global warming and changes in drought. *Nat. Clim. Change* **2014**, *4*, 17–22. [CrossRef]
2. Cook, B.I.; Mankin, J.S.; Anchukaitis, K.J. Climate change and drought: From past to future. *Curr. Clim. Change Rep.* **2015**, *4*, 164–179. [CrossRef]
3. Samaniego, L.; Thober, S.; Kumar, R.; Wanders, N.; Rakovec, O.; Pan, M.; Zink, M.; Sheffield, J.; Wood, E.F.; Marx, A. Anthropogenic warming exacerbates European soil moisture droughts. *Nat. Clim. Change* **2018**, *8*, 421–426. [CrossRef]
4. IPCC. *Climate Change 2022: Impacts, Adaptation and Vulnerability*; Intergovernmental Panel on Climate Change: Geneva, Switzerland, 2022.
5. Christensen, L.; Adams, H.R.; Tai, X.; Barnard, H.R.; Brooks, P.D. Increasing plant water stress and decreasing summer streamflow in response to a warmer and wetter climate in seasonally snow-covered forests. *Ecohydrology* **2020**, *14*, 18. [CrossRef]
6. Williams, A.P.; Cook, E.R.; Smerdon, J.E.; Cook, B.I.; Abatzoglou, J.T.; Bolles, K.; Baek, S.H.; Badger, A.M.; Livneh, B. Large contribution from anthropogenic warming to an emerging North American megadrought. *Science* **2020**, *368*, 314–318. [CrossRef] [PubMed]
7. IPCC. *Climate Change 2014: Mitigation of Climate Change*; Intergovernmental Panel on Climate Change: Geneva, Switzerland; Cambridge University Press: New York, NY, USA, 2015.
8. D'Orangeville, L.; Maxwell, J.; Kneeshaw, D.; Pederson, N.; Duchesne, L.; Logan, T.; Houle, D.; Arseneault, D.; Beier, C.M.; Bishop, D.A.; et al. Drought timing and local climate determine the sensitivity of eastern temperate forests to drought. *Glob. Change Biol.* **2015**, *24*, 2339–2351. [CrossRef]
9. Cholet, C.; Houle, D.; Sylvain, J.-D.; Doyon, F.; Maheu, A. Climate Change Increases the Severity and Duration of Soil Water Stress in the Temperate Forest of Eastern North America. *Front. For. Glob. Change* **2022**, *5*, 13. [CrossRef]
10. Lisar, S.Y.S.; Motafakkerazad1, R.; Hossain, M.M.; Rahman, I.M.M. *Water Stress in Plants: Causes, Effects and Responses In Water Stress*; Rahman, I.M.M., Hasegawa, H., Eds.; IntechOpen: London, UK, 2012.
11. Imadi, S.R.; Gul, A.; Dikilitas, M.; Karakas, S.; Sharma, I.; Ahmad, P. Water stress: Types, causes, and impact on plant growth and development. In *Water Stress and Crop Plants: A Sustainable Approach, Volume 2*; Ahmad, P., Ed.; John Wiley & Sons Ltd.: Hoboken, NJ, USA, 2016.
12. Hsiao, T.C. Plant Responses to Water Stress. *Annu. Rev. Plant Physiol.* **1973**, *24*, 519–570. [CrossRef]
13. Vaadia, Y.; Raney, F.C.; Hagan, R.M. Plant Water Deficits and Physiological Processes. *Annu. Rev. Plant Physiol.* **1961**, *12*, 265–292. [CrossRef]
14. Kramer, P.J. Water Stress and Plant Growth. *Agron. J.* **1963**, *55*, 31–35. [CrossRef]
15. Escalona, J.; Flexas, J.; Medrano, H. Stomatal and non-stomatal of photosynthesis under water stress in field grown grapevines. *Funct. Plant Biol.* **2000**, *27*, 87. [CrossRef]
16. Ordin, L. Effect of Water Stress on Cell Wall Metabolism of Avena Coleoptile Tissue. *Plant Physiol.* **1960**, *35*, 443–450. [CrossRef]
17. Jaleel, C.; Manivannan, P.; Wahid, A.; Farooq, M.; Al-Juburi, H.; Somasundaram, R.; Panneerselvam, R. Drought Stress in Plants: A Review on Morphological Characteristics and Pigments Composition. *Int. J. Agric. Biol.* **2009**, *11*, 100–105.
18. Bohnert, H.J.; Jensen, R.G. Strategies for engineering water-stress tolerance in plants. *Trend Biotechnol.* **1996**, *14*, 89–97. [CrossRef]
19. Farahani, H.A.; Valadabadi, S.A.; Daneshian, J.; Khalvati, M.A. Evaluation changing of essential oil of balm (*Melissa officinalis* L.) under water deficit stress conditions. *J. Med. Plants Res.* **2009**, *3*, 329–333.
20. Dobbertin, M.; Wermelinger, B.; Bigler, C.; Bürgi, M.; Carron, M.; Forster, B.; Gimmi, U.; Rigling, A. Linking Increasing Drought Stress to Scots Pine Mortality and Bark Beetle Infestations. *Sci. World J.* **2007**, *7*, 9. [CrossRef]
21. Wang, W.; Peng, C.; Kneeshaw, D.D.; Larocque, G.R.; Luo, Z. Drought-induced tree mortality: Ecological consequences, causes, and modeling. *Environ. Rev.* **2012**, *20*, 109–121. [CrossRef]

22. Kharuk, V.I.; Im, S.T.; Petrov, I.A.; Dvinskaya, M.L.; Fedotova, E.V.; Ranson, K.J. Fir decline and mortality in the southern Siberian Mountains. *Reg. Environ. Change* **2017**, *17*, 803–812. [CrossRef]
23. Xu, P.; Zhou, T.; Yi, C.; Luo, H.; Zhao, X.; Fang, W.; Gao, S.; Liu, X. Impacts of Water Stress on Forest Recovery and Its Interaction with Canopy Height. *Environ. Res. Public Health* **2018**, *15*, 16. [CrossRef]
24. Hardy, G.; Matusick, G.; Ruthrof, K. Impacts of large scale drought deaths in Western Australia's northern jarrah (*Eucalyptus marginata*) forest. In Proceedings of the Ecological Society of Australia, Annual Conference, Melbourne, Australia, 27–30 November 2012.
25. Matusick, G.; Ruthrof, K.X.; Brouwers, N.C.; Dell, B.; Hardy, G.S.J. Sudden forest canopy collapse corresponding with extreme drought and heat in a mediterranean-type eucalypt forest in southwestern Australia. *Eur. J. For. Res.* **2013**, *132*, 497–510. [CrossRef]
26. Zou, J.; Ding, J.; Qin, Y.; Wang, F. Response of water use efficiency of Central Asia ecosystem to drought based on remote sensing data. *Trans. Chin. Soc. Agric. Eng.* **2018**, *34*, 145–152.
27. Anderson, L.O.; Ribeiro Neto, G.; Cunha, A.P.; Fonseca, M.G.; Moura, Y.M.d.; Dalagnol, R.; Wagner, F.H.; Aragao, L.E.O.e.C.d. Vulnerability of Amazonian forests to repeated droughts. *Philos. Trans. R. Soc. B Biol. Sci.* **2018**, *373*, 20170411. [CrossRef] [PubMed]
28. Lucas, A. Water Stress and Disease Development in *Eucalyptus marginata* (Jarrah) Infected with *Phytophthora cinnamomi*. Ph.D. Dissertation, Murdoch University, Perth, Australia, 2003.
29. Zou, L.; Cao, S.; Zhao, A.; Sanchez-Azofeifa, A. Assessing the Temporal Response of Tropical Dry Forests to Meteorological Drought. *Remote Sens.* **2020**, *12*, 2341. [CrossRef]
30. Meyer, B.F.; Buras, A.; Rammig, A.; Zang, C.S. Higher susceptibility of beech to drought in comparison to oak. *Dendrochronologia* **2020**, *64*, 125780. [CrossRef]
31. Huete, A.R. Chapter 11—Remote sensing for environmental monitoring. In *Environmental Monitoring and Characterization*; Artiola, J.F., Pepper, I.L., Brusseau, M.L., Eds.; Academic Press: Cambridge, MA, USA, 2004; pp. 183–206.
32. Wang, J.; Sammis, T.W.; Gutschick, V.P.; Gebremichael, M.; Dennis, S.O.; Harrison, R.E. Review of Satellite Remote Sensing Use in Forest Health Studies. *Open Geogr. J.* **2010**, *3*, 28–42. [CrossRef]
33. Ahmad, U.; Alvino, A.; Marino, S. A Review of Crop Water Stress Assessment Using Remote Sensing. *Remote Sens.* **2021**, *13*, 4155. [CrossRef]
34. Virnodkar, S.S.; Pachghare, V.K.; Patil, V.C.; Jha, S.K. Remote sensing and machine learning for crop water stress determination in various crops: A critical review. *Precis. Agric.* **2020**, *21*, 1121–1155. [CrossRef]
35. Hansen, M.C.; Thomas, R.L. A review of large area monitoring of land cover change using Landsat data. *Remote Sens. Environ.* **2012**, *122*, 66–74. [CrossRef]
36. Zhang, Y.; Peng, C.; Li, W.; Fang, X.; Zhang, T.; Zhu, Q.; Chen, H.; Zhao, P. Monitoring and estimating drought-induced impacts on forest structure, growth, function, and ecosystem services using remote-sensing data: Recent progress and future challenges. *Environ. Rev.* **2013**, *21*, 103–115. [CrossRef]
37. Harris, A.; Bryant, R.G.; Baird, A.J. Mapping the effects of water stress on Sphagnum: Preliminary observations using airborne remote sensing. *Remote Sens. Environ.* **2006**, *100*, 363–378. [CrossRef]
38. Joshi, R.C.; Ryu, D.; Sheridan, G.J.; Lane, P.N.J. Modeling Vegetation Water Stress over the Forest from Space: Temperature Vegetation Water Stress Index (TVWSI). *Remote Sens.* **2021**, *13*, 23. [CrossRef]
39. Liu, N.; Deng, Z.; Wang, H.; Luo, Z.; Gutiérrez-Juradob, H.A.; He, X.; Guan, H. Thermal remote sensing of plant water stress in natural ecosystems. *For. Ecol. Manag.* **2020**, *476*, 14. [CrossRef]
40. Anderson, L.O.; Malhi, Y.; Aragao, L.E.O.C.; Ladle, R.; Arai, E.; Barbier, N.; Phillips, O. Remote sensing detection of droughts in Amazonian forest canopies. *New Phytol.* **2010**, *187*, 733–750. [CrossRef]
41. Govender, M.; Dye, P.J.; Weiersbye, I.M.; Witkowski, E.T.F.; Ahmed, F. Review of commonly used remote sensing and ground-based technologies to measure plant water stress. *Water SA* **2009**, *35*, 741–752. [CrossRef]
42. Clay, D.; Kim, K.-i.; Chang, J.; Clay, S.; Dalsted, K. Characterizing Water and Nitrogen Stress in Corn Using Remote Sensing. *Agron. J.* **2006**, *98*, 579–587. [CrossRef]
43. Cohen, W.B. Response Of Vegetation Indices To Changes In Three Measures Of Leaf Water Stress. *Photogramm. Eng. Remote Sens.* **1991**, *57*, 195–202.
44. Sepulcre-Cantó, G.; Zarco-Tejada, P.J.; Jiménez-Muñoz, J.C.; Sobrino, J.A.; de Miguel, E.; Villalobos, F.J. Detection of water stress in an olive orchard with thermal remote sensing imagery. *Agric. For. Meteorol.* **2006**, *136*, 31–44. [CrossRef]
45. Gausman, H.W. Reflectance of leaf components. *Remote Sens. Environ.* **1977**, *6*, 1–9. [CrossRef]
46. Ceccato, P.; Flasse, S.; Tarantola, S.; Jacquemoud, S.; Grégoire, J.-M. Detecting vegetation leaf water content using reflectance in the optical domain. *Remote Sens. Environ.* **2001**, *77*, 22–33. [CrossRef]
47. Zhang, F.; Zhou, G. Estimation of vegetation water content using hyperspectral vegetation indices: A comparison of crop water indicators in response to water stress treatments for summer maize. *BMC Ecol.* **2019**, *19*, 12. [CrossRef]
48. Coops, N.; Stone, C.; Culvenor, D.S.; Chisholm, L.A.; Merton, R.N. Chlorophyll content in eucalypt vegetation at the leaf and canopy scales as derived from high resolution spectral data. *Tree Physiol.* **2003**, *23*, 23–31. [CrossRef] [PubMed]
49. Curran, P.J.; Dungan, J.L.; Gholz, H.L. Exploring the relationship between reflectance red edge and chlorophyll content in slash pine. *Tree Physiol.* **1990**, *7*, 33–48. [CrossRef] [PubMed]

50. Stone, C.; Chisholm, L.; Coops, N. Spectral reflectance characteristics of eucalypt foliage damaged by insects. *Aust. J. Bot.* **2001**, *49*, 687–698. [CrossRef]
51. Blackburn, G.A. Relationships between Spectral Reflectance and Pigment Concentrations in Stacks of Deciduous Broadleaves. *Remote Sens. Environ.* **1999**, *70*, 224–237. [CrossRef]
52. Rouse, J.W.; Haas, R.H.; Schell, J.A.; Deering, D.W. Monitoring Vegetation Systems in the Great Plains with Erts. *Nasa Spec. Publ.* **1974**, *351*, 309–317.
53. Lichtenthaler, H.K. Chlorophylls and Carotenoids: Pigments of Photosynthetic Biomembranes. *Methods Enzymol.* **1987**, *148*, 350–382. [CrossRef]
54. Faurtyot, T.; Baret, F. Vegetation water and dry matter contents estimated from top-of-the-atmosphere reflectance data: A simulation study. *Remote Sens. Environ.* **1997**, *61*, 34–45. [CrossRef]
55. Asner, G.P. Biophysical and Biochemical Sources of Variability in Canopy Reflectance. *Remote Sens. Environ.* **1998**, *64*, 234–253. [CrossRef]
56. Coops, N.; Dury, S.; Smith, M.-L.; Martin, M.; Ollinger, S. Comparison of green leaf eucalypt spectra using spectral decomposition. *Aust. J. Bot.* **2002**, *50*, 567–576. [CrossRef]
57. Curran, P.J.; Dungan, J.L.; Macler, B.A.; Plummer, S.E. The effect of a red leaf pigment on the relationship between red edge and chlorophyll concentration. *Remote Sens. Environ.* **1991**, *35*, 69–76. [CrossRef]
58. Laskari, M.; Menexes, G.; Kalfas, I.; Gatzolis, I.; Dordas, C. Water Stress Effects on the Morphological, Physiological Characteristics of Maize (*Zea mays* L.), and on Environmental Cost. *Agron. J.* **2022**, *12*, 2386. [CrossRef]
59. Eitel, J.U.H.; Gessler, P.E.; Smith, A.M.S.; Robberecht, R. Suitability of existing and novel spectral indices to remotely detect water stress in *Populus* spp. *For. Ecol. Manag.* **2006**, *229*, 170–182. [CrossRef]
60. Fuchs, M. Infrared measurement of canopy temperature and detection of plant water stress. *Theor. Appl. Climatol.* **1990**, *42*, 253–261. [CrossRef]
61. Kurihara, J.; Koo, V.-C.; Guey, C.W.; Lee, Y.P.; Abidin, H. Early Detection of Basal Stem Rot Disease in Oil Palm Tree Using Unmanned Aerial Vehicle-Based Hyperspectral Imaging. *Remote Sens.* **2022**, *14*, 10. [CrossRef]
62. García-Tejero, I.F.; Gutiérrez-Gordillo, S.; Ortega-Arévalo, C.; Iglesias-Contreras, M.; Moreno, J.M.; Souza-Ferreira, L.; Durán-Zuazo, V.H. Thermal imaging to monitor the crop-water status in almonds by using the non-water stress baselines. *Sci. Hortic.* **2018**, *238*, 91–97. [CrossRef]
63. Farooq, M.; Wahid, A.; Kobayashi, N.; Fujita, D.; Basra, S.M.A. Plant drought stress: Effects, mechanisms and management. *J. Plant Physiol.* **2009**, *165*, 133–151. [CrossRef]
64. Pirzad, A.; Shakiba, M.R.; Zehtab-Salmasi, S.; Mohammadi, S.A.; Darvishzadeh, R.; Samadi, A. Effect of water stress on leaf relative water content, chlorophyll, proline and soluble carbohydrates in *Matricaria chamomilla* L. *J. Med. Plants Res.* **2011**, *5*, 2483–2488.
65. Rolando, C.A.; Little, K.M. Using chlorophyll fluorescence to determine stress in Eucalyptus grandis seedlings. *S. Afr. For. J.* **2003**, *197*, 5–12. [CrossRef]
66. Surendar, K.; Devi, D.; Ravi, I.; Jeyakumar, P.; Velayudham, K. Effect of Water Stress on Leaf Temperature, Transpiration Rate, Stomatal Diffusive Resistance and Yield of Banana. *Plant Gene Trait.* **2013**, *4*, 43–47. [CrossRef]
67. Govindjee; Downton, W.J.S.; Fork, D.C.; Armond, P.A. Chlorophyll A fluorescence transient as an indicator of water potential of leaves. *Plant Sci. Lett.* **1981**, *20*, 191–194. [CrossRef]
68. Lichtenthaler, H.K.; Buschmann, C.; Rinderle, U.; Schmuck, G. Application of chlorophyll fluorescence in ecophysiology. *Radiat. Environ. Biophys.* **1996**, *25*, 297–308. [CrossRef] [PubMed]
69. Jordan, C.F. Derivation of Leaf-Area Index from Quality of Light on the Forest Floor. *Ecology* **1969**, *50*, 663–666. [CrossRef]
70. Huete, A.R. A soil-adjusted vegetation index (SAVI). *Remote Sens. Environ.* **1988**, *25*, 295–309. [CrossRef]
71. Huete, A.; Didan, K.; Miura, T.; Rodriguez, E.P.; Gao, X.; Ferreira, L.G. Overview of the radiometric and biophysical performance of the MODIS vegetation indices. *Remote Sens. Environ.* **2002**, *83*, 195–213. [CrossRef]
72. Gabban, A.; San-Miguel-Ayanz, J.; Barbosa, P.; Libertà, G. Analysis of NOAA-AVHRR NDVI inter-annual variability for forest fire risk estimation. *Int. J. Remote Sens.* **2006**, *27*, 1725–1732. [CrossRef]
73. Ghulam, A.; Qin, Q.; Zhan, Z. Designing of the perpendicular drought index. *Environ. Geol.* **2006**, *52*, 1045–1052. [CrossRef]
74. Ghulam, A.; Qin, Q.; Teyip, T.; Li, Z. Modified perpendicular drought index (MPDI): A real-time drought monitoring method. *ISPRS J. Photogramm. Remote Sens.* **2007**, *62*, 150–164. [CrossRef]
75. Hunt, E.R.; Rock, B.N.; Nobel, P.S. Measurement of leaf relative water content by infrared reflectance. *Remote Sens. Environ.* **1987**, *22*, 429–435. [CrossRef]
76. Gao, B.-c. A normalized difference water index for remote sensing of vegetation liquid water from space—NDWI. *Remote Sens. Environ.* **1996**, *58*, 257–266. [CrossRef]
77. Fensholt, R.; Sandholt, I. Derivation of a shortwave infrared water stress index from MODIS near- and shortwave infrared data in a semiarid environment. *Remote Sens. Environ.* **2003**, *87*, 111–121. [CrossRef]
78. Maki, M.; Ishiahra, M.; Tamura, M. Estimation of leaf water status to monitor the risk of forest fires by using remotely sensed data. *Remote Sens. Environ.* **2004**, *90*, 441–450. [CrossRef]
79. Jang, J.-D.; Viau, A.A.; Anctil, F. Thermal-water stress index from satellite images. *Int. J. Remote Sens.* **2006**, *27*, 1619–1639. [CrossRef]

80. Gamon, J.A.; Peñuelas, J.; Field, C.B. A narrow-waveband spectral index that tracks diurnal changes in photosynthetic efficiency. *Remote Sens. Environ.* **1992**, *41*, 35–44. [CrossRef]
81. Gitelson, A.A.; Kaufman, Y.J.; Merzlyak, M.N. Use of a green channel in remote sensing of global vegetation from EOS-MODIS. *Remote Sens. Environ.* **1996**, *58*, 289–298. [CrossRef]
82. Carlson, T.N.; Ripley, D.A. On the relation between NDVI, fractional vegetation cover, and leaf area index. *Remote Sens. Environ.* **1997**, *62*, 241–252. [CrossRef]
83. Gitelson, A.A.; Gritz, Y.; Merzlyak, M.N. Relationships between leaf chlorophyll content and spectral reflectance and algorithms for non-destructive chlorophyll assessment in higher plant leaves. *J. Plant Physiol.* **2003**, *160*, 271–282. [CrossRef]
84. Gamon, J.; Serrano, L.; Surfus, J. The photochemical reflectance index: An optical indicator of photosynthetic radiation use efficiency across species, functional types, and nutrient levels. *Oecologia* **1997**, *112*, 492–501. [CrossRef]
85. Sukhova, E.; Sukhov, V. Relation of Photochemical Reflectance Indices Based on Different Wavelengths to the Parameters of Light Reactions in Photosystems I and II in Pea Plants. *Remote Sens.* **2020**, *12*, 24. [CrossRef]
86. Zhang, C.; Filella, I.; Garbulsky, M.F.; Peñuelas, J. Affecting Factors and Recent Improvements of the Photochemical Reflectance Index (PRI) for Remotely Sensing Foliar, Canopy and Ecosystemic Radiation-Use Efficiencies. *Remote Sens.* **2016**, *8*, 677. [CrossRef]
87. Jackson, R.D.; Idso, S.B.; Reginato, R.J.; Pinter, P.J. Canopy temperature as a crop water stress indicator. *Water Resour. Res.* **1981**, *17*, 1133–1138. [CrossRef]
88. Moran, M.S.; Clarke, T.R.; Inoue, Y.; Vidal, A. Estimating crop water deficit using the relation between surface-air temperature and spectral vegetation index. *Remote Sens. Environ.* **1994**, *49*, 246–263. [CrossRef]
89. Carlson, T.N.; Gillies, R.R.; Perry, E.M. A method to make use of thermal infrared temperature and NDVI measurements to infer surface soil water content and fractional vegetation cover. *Remote Sens. Rev.* **1994**, *52*, 45–59. [CrossRef]
90. Wang, P.-x.; Li, X.-w.; Gong, J.-y.; Song, C. Vegetation temperature condition index and its application for drought monitoring. In Proceedings of the Geoscience and Remote Sensing Symposium, Sydney, NSW, Australia, 9–13 July 2002.
91. Sandholt, I.; Rasmussen, K.; Andersen, J. A simple interpretation of the surface temperature/vegetation index space for assessment of surface moisture status. *Remote Sens. Environ.* **2002**, *79*, 213–224. [CrossRef]
92. Shakya, N.; Yamaguchi, Y. Vegetation, water and thermal stress index for study of drought in Nepal and central northeastern India. *Int. J. Remote Sens.* **2010**, *31*, 903–912. [CrossRef]
93. Wu, M.; Lu, H. A modified vegetation water supply index (MVWSI) and its application in drought monitoring over Sichuan and Chongqing, China. *J. Integr. Agric.* **2016**, *15*, 2132–2141. [CrossRef]
94. Amani, M.; Salehi, B.; Mahdavi, S.; Masjedi, A.; Dehnavi, S. Temperature-Vegetation-soil Moisture Dryness Index (TVMDI). *Remote Sens. Environ.* **2017**, *197*, 1–14. [CrossRef]
95. Gitelson, A.A.; Merzlyak, M.N. Signature Analysis of Leaf Reflectance Spectra: Algorithm Development for Remote Sensing of Chlorophyll. *J. Plant Physiol.* **1996**, *148*, 494–500. [CrossRef]
96. Zarco-Tejada, P.J.; Miller, J.R.; Mohammed, G.H.; Noland, T.L. Chlorophyll Fluorescence Effects on Vegetation Apparent Reflectance: I. Leaf-Level Measurements and Model Simulation. *Remote Sens. Environ.* **2000**, *74*, 582–595. [CrossRef]
97. Gitelson, A.A.; Zur, Y.; Chivkunova, O.B.; Merzlyak, M.N. Assessing carotenoid content in plant leaves with reflectance spectroscopy. *Plant Physiol. Biochem.* **2002**, *75*, 272–281. [CrossRef]
98. Datt, B. A New Reflectance Index for Remote Sensing of Chlorophyll Content in Higher Plants: Tests using Eucalyptus Leaves. *J. Plant Physiol.* **1999**, *154*, 30–36. [CrossRef]
99. Peñuelas, J.; Gamon, J.A.; Fredeen, A.L.; Merino, J.; Field, C.B. Reflectance indices associated with physiological changes in nitrogen- and water-limited sunflower leaves. *Remote Sens. Environ.* **1994**, *48*, 135–146. [CrossRef]
100. Musick, H.B.; Pelletier, R.E. Response to soil moisture of spectral indexes derived from bidirectional reflectance in thematic mapper wavebands. *Remote Sens. Environ.* **1988**, *25*, 167–184. [CrossRef]
101. Hunt, E.R., Jr.; Rock, B.N. Detection of changes in leaf water content using near- and middle-infrared reflectances. *Remote Sens. Environ.* **1989**, *30*, 43–54. [CrossRef]
102. Tucker, C.J. Remote sensing of leaf water content in the near infrared. *Remote Sens. Environ.* **1980**, *10*, 23–32. [CrossRef]
103. Pu, R.; Ge, S.; Kelly, N.M.; Gong, P. Spectral absorption features as indicators of water status in coast live oak (*Quercus agrifolia*) leaves. *Int. J. Remote Sens.* **2003**, *24*, 1799–1810. [CrossRef]
104. Jackson, T.J.; Chen, D.; Cosh, M.; Li, F.; Anderson, M.; Walthall, C.; Doriaswamy, P.; Hunt, E.R. Vegetation water content mapping using Landsat data derived normalized difference water index for corn and soybeans. *Remote Sens. Environ.* **2004**, *92*, 475–482. [CrossRef]
105. Carroll, D.A.; Hansen, N.C.; Hopkins, B.G.; DeJonge, K.C. Leaf temperature of maize and Crop Water Stress Index with variable irrigation and nitrogen supply. *Irrig. Sci.* **2017**, *35*, 549–560. [CrossRef]
106. Zhang, R.; Zhou, Y.; Yue, Z.; Chen, X.; Cao, X.; Ai, X.; Jiang, B.; Xing, Y. The leaf-air temperature difference reflects the variation in water status and photosynthesis of sorghum under waterlogged conditions. *PLoS ONE* **2019**, *14*, e0219209. [CrossRef]
107. Jackson, R.D. Canopy Temperature and Crop Water Stress. *Adv. Irrig.* **1982**, *1*, 43–85. [CrossRef]
108. Shahenshah; Isoda, A. Effects of Water Stress on Leaf Temperature and Chlorophyll Fluorescence Parameters in Cotton and Peanut. *Plant Prod. Sci.* **2010**, *13*, 269–278. [CrossRef]
109. Netto, A.T.; Campostrini, E.; de Oliveira, J.G.; Bressan-Smith, R.E. Photosynthetic pigments, nitrogen, chlorophyll a fluorescence and SPAD-502 readings in coffee leaves. *Sci. Hortic.* **2005**, *104*, 199–209. [CrossRef]

110. Ma, H.; Cui, T.; Cao, L. Monitoring of Drought Stress in Chinese Forests Based on Satellite Solar-Induced Chlorophyll Fluorescence and Multi-Source Remote Sensing Indices. *Remote Sens.* **2023**, *15*, 879. [CrossRef]
111. Pandiyan, S.; Navaneethan, C.; Vijayan, R.; Gunasekaran, G.; Khan, K.Y.; Guo, Y. Evaluation of drought using satellite solar-induced chlorophyll fluorescence during crop development stage over Xinjiang, China. *Measurement* **2021**, *187*, 11032. [CrossRef]
112. Kior, A.; Sukhov, V.; Sukhova, E. Application of Reflectance Indices for Remote Sensing of Plants and Revealing Actions of Stressors. *Photonics* **2021**, *8*, 27. [CrossRef]
113. Maxwell, K.; Johnson, G.N. Chlorophyll fluorescence—A practical guide. *J. Exp. Bot.* **2000**, *51*, 659–668. [CrossRef] [PubMed]
114. Millard, J.P.; Jackson, R.D.; Goettelman, R.C.; Reginato, R.J.; Idso, S.B. Crop water-stress assessment using an airborne thermal scanner. *Photogramm. Eng. Remote Sens.* **1978**, *44*, 77–85.
115. Goillot, C.C. Airborne thermography or infrared remote sensing. *Bibl. Radiol.* **1975**, *6*, 237–248.
116. Katimbo, A.; Rudnick, D.R.; DeJonge, K.C.; Lo, T.H.; Qiao, X.; Franz, T.E.; Nakabuye, H.N.; Duan, J. Crop water stress index computation approaches and their sensitivity to soil water dynamics. *Agric. Water Manag.* **2022**, *266*, 107575. [CrossRef]
117. Burrows, N.; Baker, P.; Harper, R.; Silberstein, R. A report on Silvicultural Guidelines 2033 Forest Management Plan for the Western Australian Department of Biodiversity, Conservation and Attractions. Available online: https://www.dbca.wa.gov.au/sites/default/files/2022-10/Independent%20Silviculture%20Review%20Panel%20Report%20May%202022.pdf (accessed on 18 November 2022).
118. Gavinet, J.; Ourcival, J.M.; Gauzere, J.; De Jalón, L.G.; Limousin, J.M. Drought mitigation by thinning; Benefits from the stem to the stand along 15 years of experimental rainfall exclusion in a holm oak coppice. *For. Ecol. Manag.* **2020**, *473*, 10. [CrossRef]
119. Liu, N.; Harper, R.J.; Smettem, K.R.J.; Dell, B.; Liu, S. Responses of streamflow to vegetation and climate change in southwestern Australia. *J. Hydrol.* **2019**, *572*, 761–770. [CrossRef]
120. Yu, P.; Zhou, T.; Luo, H.; Liu, X.; Shi, P.; Zhao, X.; Xiao, Z.; Zhang, Y.; Zhou, P. Interannual variation of gross primary production detected from optimal convolutional neural network at multi-timescale water stress. *Remote Sens. Ecol. Conserv.* **2022**, *8*, 409–425. [CrossRef]
121. Sang, Z.; Hamann, A. Climatic limiting factors of North American ecosystems: A remote-sensing based vulnerability analysis. *Environ. Res. Lett.* **2022**, *17*, 094011. [CrossRef]
122. Lyons, D.S.; Dobrowski, S.Z.; Holden, Z.A.; Maneta, M.P.; Sala, A. Soil moisture variation drives canopy water content dynamics across the western US. *Remote Sens. Environ.* **2020**, *253*, 112233. [CrossRef]
123. Ji, Y.; Li, Y.; Yao, N.; Biswas, A.; Zou, Y.; Meng, Q.; Liu, F. The lagged effect and impact of soil moisture drought on terrestrial ecosystem water use efficiency. *Ecol. Indic.* **2021**, *133*, 108349. [CrossRef]
124. Przeździecki, K.; Zawadzki, J.J.; Urbaniak, M.; Ziemblińska, K.; Miatkowski, Z. Using temporal variability of land surface temperature and normalized vegetation index to estimate soil moisture condition on forest areas by means of remote sensing. *Ecol. Indic.* **2023**, *148*, 110088. [CrossRef]
125. Ghasempour, R.; Aalami, M.T.; Kirca, V.S.O.; Roushangar, K. Remote sensing-based drought severity modeling and mapping using multiscale intelligence methods. *Stoch. Environ. Res. Risk Assess.* **2023**, *37*, 889–902. [CrossRef]
126. Korner, C. Humidity responses in forest trees: Precautions in thermal scanning surveys. *Arch. Meteorol. Geophys. Bioclimatol. B* **1985**, *36*, 83–96. [CrossRef]
127. Spencer, R.D. Large-scale aerial photo comparison for detecting pine dieback. *Aust. For.* **1985**, *48*, 102–108. [CrossRef]
128. Running, S.W.; Nemani, R.R. Relating seasonal patterns of the AVHRR vegetation index to simulated photosynthesis and transpiration of forests in different climates. *Remote Sens. Environ.* **1988**, *24*, 347–367. [CrossRef]
129. Pierce, L.L.; Running, S.W.; Riggs, G.A. Remote detection of canopy water stress in coniferous forests using the NS001 thematic mapper simulator and the thermal infrared multispectral scanner. *PE&RS Photogramm. Eng. Remote Sens.* **1990**, *56*, 579–586.
130. Cohen, W.B. Temporal versus spatial variation in leaf reflectance under changing water stress conditions. *Int. J. Remote Sens.* **1991**, *12*, 1865–1876. [CrossRef]
131. Riggs, G.A.; Running, S.W. Detection Of Canopy Water-Stress In Conifers Using The Airborne Imaging Spectrometer. *Remote Sens. Environ.* **1991**, *35*, 51–68. [CrossRef]
132. Kalluri, S.N.V.; Doraiswamy, P. Modeling transpiration and water stress in vegetation from satellite and ground measurements. In Proceedings of the 1995 International Geoscience and Remote Sensing Symposium (IGARSS 95), Florence, Italy, 10–14 July 1995; pp. 1483–1487.
133. Vidal, A.; Devauxros, C. Evaluating Forest-Fire Hazard With A Landsat Tm Derived Water-Stress Index. *Agric. For. Meteorol.* **1995**, *77*, 207–224. [CrossRef]
134. Gunther, K.P.; Dahn, H.G.; Ludeker, W. Remote-Sensing Vegetation Status By Laser-Induced Fluorescence. *Remote Sens. Environ.* **1994**, *47*, 10–17. [CrossRef]
135. Valentini, R.; Cecchi, G.; Mazzinghi, P.; Mugnozza, G.S.; Agati, G.; Bazzani, M.; Deangelis, P.; Fusi, F.; Matteucci, G.; Raimondi, V. Remote-sensing of chlorophyll-a fluorescence of vegetation canopies.2. Physiological significance of fluorescence signal in response to environmental stresses. *Remote Sens. Environ.* **1994**, *47*, 29–35. [CrossRef]
136. Buschmann, C.; Schweiger, J.; Lichtenthaler, H.K.; Richter, P. Application of the Karlsruhe CCD-OMA LIDAR-fluorosensor in stress detection of plants. *J. Plant Physiol.* **1996**, *148*, 548–554. [CrossRef]

137. Lichtenthaler, H.K.; Subhash, N.; Wenzel, O.; Miehe, J.A.; IEEE. Laser-induced imaging of blue/red and blue/far-red fluorescence ratios, F440/F690 and F440/F740, as a means of early stress detection in plants. In Proceedings of the 1997 International Geoscience and Remote Sensing Symposium (IGARSS 97) on Remote Sensing—A Scientific Vision for Sustainable Development, Singapore, 3–8 August 1997; pp. 1799–1801.
138. Illera, P.; Delgado, J.A.; Unzueta, A.F.; Manso, A.A.F. Integration of NOAA-AVHRR and meteorological data in a GIS—Application for vegetation monitoring in Castilla y Leon, Spain. In Proceedings of the 19th EARSeL Symposium on Remote Sensing in the 21st Century, Valladolid, Spain, 31 May–2 June 1999; pp. 47–54.
139. Illera, P.; Fernandez, A.; Calle, A. Operational forest fire danger indices derived from NOAA images. In *Remote Sensing'96: Integrated Applications for Risk Assessment and Disaster Prevention for the Mediterranean: Proceedings of the 16th EARSel Symposium on Integrated Applications for Risk Assessment and Disaster Prevention for the Mediterranean, Malta, 20–23 May 1996*; A A Balkema Publishers: London, UK, 1997; pp. 319–325.
140. Illera, P.; Fernandez, A.; Delgado, J.A. Temporal evolution of the NDVI as an indicator of forest fire danger. *Int. J. Remote Sens.* **1996**, *17*, 1093–1105. [CrossRef]
141. Karlikowski, T.; Dabrowska-Zieliska, K.; Zawila-Niedzwiecki, T.; Gruszczynska, M.; Santorski, Z.; Sakowska, H.; Janowska, M. The use of NOAA-AVHRR images for forest fire risk assessment. *Pr. Inst. Badaw. Lesn.* **1997**, *72*, 72.
142. Deshayes, M.; Guyon, D.; Jeanjean, H.; Stach, N.; Jolly, A.; Hagolle, O. The contribution of remote sensing to the assessment of drought effects in forest ecosystems. *Ann. For. Sci.* **2006**, *63*, 579–595. [CrossRef]
143. Penuelas, J.; Llusia, J.; Pinol, J.; Filella, I. Photochemical reflectance index and leaf photosynthetic radiation-use-efficiency assessment in Mediterranean trees. *Int. J. Remote Sens.* **1997**, *18*, 2863–2868. [CrossRef]
144. Penuelas, J.; Pinol, J.; Ogaya, R.; Filella, I. Estimation of plant water concentration by the reflectance water index WI (R900/R970). *Int. J. Remote Sens.* **1997**, *18*, 2869–2875. [CrossRef]
145. Asner, G.P.; Nepstad, D.; Cardinot, G.; Ray, D. Drought stress and carbon uptake in an Amazon forest measured with spaceborne imaging spectroscopy. *Proc. Natl. Acad. Sci. USA* **2004**, *101*, 6039–6044. [CrossRef]
146. Harding, L.W.; Miller, W.D.; Swift, R.N.; Wright, C.W. Aircraft Remote Sensing. In *Encyclopedia of Ocean Sciences*, 2nd ed.; Academic Press: Cambridge, MA, USA, 2001; pp. 138–146.
147. Gobron, N.; Pinty, B.; Mélin, F.; Taberner, M.; Verstraete, M.M.; Belward, A.; Lavergne, T.; Widlowski, L. The state of vegetation in Europe following the 2003 drought. *Int. J. Remote Sens.* **2005**, *26*, 2013–2020. [CrossRef]
148. Gonzalez-Alonso, F.; Merino-de-Miguel, S.; Cuevas, J.M.; Roldan-Zamarron, A.; Garcia-Gigorro, S.; Calle, A.; Casanova, J.L.; Romo, A. Previous Drought Conditions and Losses Produced at the Valencia de Alcantara Forest Fire in August 2003. In *New strategies for European Remote Sensing, Proceedings of the 24th Symposium of the European Association of Remote Sensing Laboratories, Dubrovnik, Croatia, 25–27 May 2004*; Millpress Science: Rotterdam, The Netherlands, 2005; pp. 95–99.
149. Leblon, B. Monitoring forest fire danger with remote sensing. *Nat. Hazards* **2005**, *35*, 343–359. [CrossRef]
150. Reichstein, M.; Ciais, P.; Papale, D.; Valentini, R.; Running, S.; Viovy, N.; Cramer, W.; Granier, A.; Ogee, J.; Allard, V.; et al. Reduction of ecosystem productivity and respiration during the European summer 2003 climate anomaly: A joint flux tower, remote sensing and modelling analysis. *Glob. Change Biol.* **2007**, *13*, 634–651. [CrossRef]
151. Gouveia, C.; Trigo, R.M.; DaCamara, C.C. Drought and vegetation stress monitoring in Portugal using satellite data. *Nat. Hazards Earth Syst. Sci.* **2009**, *9*, 185–195. [CrossRef]
152. Wang, C.; Lu, Z.; Haithcoat, T.L. Using Landsat images to detect oak decline in the Mark Twain National Forest, Ozark Highlands. *For. Ecol. Manag.* **2007**, *240*, 70–78. [CrossRef]
153. Lu, X.; Zhuang, Q. Evaluating evapotranspiration and water-use efficiency of terrestrial ecosystems in the conterminous United States using MODIS and AmeriFlux data. *Remote Sens. Environ.* **2010**, *114*, 1924–1939. [CrossRef]
154. Wang, L.; Luo, Y.Q.; Huang, H.G.; Shi, J.; Keliövaara, K.; Teng, W.X.; Qi, G.X. Reflectance features of water stressed Larix gmelinii needles. *For. Stud. China* **2009**, *11*, 28–33. [CrossRef]
155. Jiang, Z.; Li, L.; Ustin, S.L. Estimation of canopy water content with MODIS spectral index. In Proceedings of the SPIE—The International Society for Optical Engineering, San Diego, CA, USA, 3–4 August 2009.
156. Goerner, A.; Reichstein, M.; Rambal, S. Tracking seasonal drought effects on ecosystem light use efficiency with satellite-based PRI in a Mediterranean forest. *Remote Sens. Environ.* **2009**, *113*, 1101–1111. [CrossRef]
157. Moreno, A.; Maselli, F.; Gilabert, M.A.; Chiesi, M.; Martinez, B.; Seufert, G. Assessment of MODIS imagery to track light-use efficiency in a water-limited Mediterranean pine forest. *Remote Sens. Environ.* **2012**, *123*, 359–367. [CrossRef]
158. Gilabert, M.A.; Moreno, A.; Maselli, F.; Chiesi, M.; Martinez, B.; Seufert, G.; Melia, J. Tracking Seasonal Drought Effects On Ecosystem Light Use Efficiency In A Mediterranean Forest Using Climatic And Remote Sensing Data. In Proceedings of the IEEE International Geoscience and Remote Sensing Symposium (IGARSS), Munich, Germany, 22–27 July 2012; pp. 1147–1150.
159. Ishimura, A.; Shimizu, Y.; Rahimzadeh-Bajgiran, P.; Omasa, K. Remote sensing of Japanese beech forest decline using an improved Temperature Vegetation Dryness Index (iTVDI). *IForest* **2011**, *4*, 195–199. [CrossRef]
160. Byer, S.; Jin, Y. Detecting Drought-Induced Tree Mortality in Sierra Nevada Forests with Time Series of Satellite Data. *Remote Sens.* **2017**, *9*, 929. [CrossRef]
161. Brouwers, N.C.; van Dongen, R.; Matusick, G.; Coops, N.C.; Strelein, G.; Hardy, G. Inferring drought and heat sensitivity across a Mediterranean forest region in southwest Western Australia: A comparison of approaches. *Forestry* **2015**, *88*, 454–464. [CrossRef]

162. Luo, H.; Zhou, T.; Wu, H.; Zhao, X.; Wang, Q.; Gao, S.; Li, Z. Contrasting Responses of Planted and Natural Forests to Drought Intensity in Yunnan, China. *Remote Sens.* **2016**, *8*, 635. [CrossRef]
163. Lee, J.E.; Frankenberg, C.; Tol, C.v.d.; Berry, J.A.; Guanter, L.; Boyce, C.K.; Fisher, J.B.; Morrow, E.; Worden, J.R.; Asefi, S.; et al. Forest productivity and water stress in Amazonia: Observations from GOSAT chlorophyll fluorescence. *Proc. R. Soc. B Biol. Sci.* **2013**, *280*, 20130171. [CrossRef]
164. Stone, C.; Penman, T.; Turner, R. Managing drought-induced mortality in Pinus radiata plantations under climate change conditions: A local approach using digital camera data. *For. Ecol. Manag.* **2012**, *265*, 94–101. [CrossRef]
165. Buddenbaum, H.; Hientgen, J.; Dotzler, S.; Werner, W.; Hill, J. A BiomeBGC-based evaluation of dryness stress of central European forests. *Int. Arch. Photogramm. Remote Sens. Spat. Inf. Sci.* **2015**, *XL-7/W3*, 345–351. Available online: https://isprs-archives.copernicus.org/articles/XL-7-W3/345/2015/ (accessed on 18 November 2022). [CrossRef]
166. Su, B.; Xue, J.; Xie, C.; Fang, Y.; Song, Y.; Fuentes, S. Digital surface model applied to unmanned aerial vehicle based photogrammetry to assess potential biotic or abiotic effects on grapevine canopies. *Int. J. Agric. Biol. Eng.* **2016**, *9*, 119–130. [CrossRef]
167. Ludovisi, R.; Tauro, F.; Salvati, R.; Khoury, S.; Mugnozza, G.S.; Harfouche, A. UAV-Based Thermal Imaging for High-Throughput Field Phenotyping of Black Poplar Response to Drought. *Front. Plant Sci.* **2017**, *8*, 1681. [CrossRef]
168. Gomez-Candon, D.; Virlet, N.; Labbe, S.; Jolivot, A.; Regnard, J.L. Field phenotyping of water stress at tree scale by UAV-sensed imagery: New insights for thermal acquisition and calibration. *Precis. Agric.* **2016**, *17*, 786–800. [CrossRef]
169. Steele-Dunne, S.C.; Friesen, J.; van de Giesen, N. Using Diurnal Variation in Backscatter to Detect Vegetation Water Stress. *Ieee Trans. Geosci. Remote Sens.* **2012**, *50*, 2618–2629. [CrossRef]
170. Konings, A.G.; Yu, Y.; Xu, L.; Yang, Y.; Schimel, D.S.; Saatchi, S.S. Active microwave observations of diurnal and seasonal variations of canopy water content across the humid African tropical forests. *Geophys. Res. Lett.* **2017**, *44*, 2290–2299. [CrossRef]
171. Vreugdenhil, M.; Greimeister-Pfeil, I.; Preimesberger, W.; Camici, S.; Dorigo, W.; Enenkel, M.; van der Schalie, R.; Steele-Dunne, S.; Wagner, W. Microwave remote sensing for agricultural drought monitoring: Recent developments and challenges. *Front. Water* **2022**, *4*. Available online: https://www.frontiersin.org/journals/water/articles/10.3389/frwa.2022.1045451/full (accessed on 18 November 2022). [CrossRef]
172. Sun, S.; Sun, G.; Caldwell, P.; McNulty, S.G.; Cohen, E.; Xiao, J.; Zhang, Y. Drought impacts on ecosystem functions of the U.S. National Forests and Grasslands: Part I evaluation of a water and carbon balance model. *For. Ecol. Manag.* **2015**, *353*, 260–268. [CrossRef]
173. Nydick, K.R.; Stephenson, N.L.; Ambrose, A.R.; Asner, G.P.; Baxter, W.L.; Das, A.J.; Dawson, T.; Martin, R.E.; Paz-Kagan, T. Leaf to landscape responses of giant sequoia to hotter drought: An introduction and synthesis for the special section. *For. Ecol. Manag.* **2018**, *419*, 249–256. [CrossRef]
174. Martin, R.E.; Asner, G.P.; Francis, E.; Ambrose, A.; Baxter, W.; Das, A.J.; Vaughn, N.R.; Paz-Kagan, T.; Dawson, T.; Nydick, K.; et al. Remote measurement of canopy water content in giant sequoias (*Sequoiadendron giganteum*) during drought. *For. Ecol. Manag.* **2018**, *419*, 279–290. [CrossRef]
175. Paz-Kagan, T.; Asner, G.P. Drivers of woody canopy water content responses to drought in a Mediterranean-type ecosystem. *Ecol. Appl.* **2017**, *27*, 2220–2233. [CrossRef]
176. Miranda, A.; Lara, A.; Altamirano, A.; Di Bella, C.; González, M.E.; Julio Camarero, J. Forest browning trends in response to drought in a highly threatened mediterranean landscape of South America. *Ecol. Indic.* **2020**, *115*, 106401. [CrossRef]
177. Qi, Y.; Zeng, Z.C. Weak Response of Vegetation Photosynthesis to Meteorological Droughts in Southwest China: Insights from Gome-2 Solar-Induced Fluorescence. In Proceedings of the International Geoscience and Remote Sensing Symposium (IGARSS), Waikoloa, HI, USA, 26 September–2 October 2020; pp. 4995–4998.
178. Schuldt, B.; Buras, A.; Arend, M.; Vitasse, Y.; Beierkuhnlein, C.; Damm, A.; Gharun, M.; Grams, T.E.E.; Hauck, M.; Hajek, P.; et al. A first assessment of the impact of the extreme 2018 summer drought on Central European forests. *Basic Appl. Ecol.* **2020**, *45*, 86–103. [CrossRef]
179. Sturm, J.; Santos, M.J.; Schmid, B.; Damm, A. Satellite data reveal differential responses of Swiss forests to unprecedented 2018 drought. *Glob. Change Biol.* **2022**, *28*, 2956–2978. [CrossRef] [PubMed]
180. Avetisyan, D. A satellite-based modified plant senescence reflectance index for green-water drought monitoring. In Proceedings of the SPIE—The International Society for Optical Engineering, Online, 13–17 September 2021.
181. Merzlyak, M.N.; Gitelson, A.A.; Chivkunova, O.B.; Rakitin, V.Y. Non-destructive optical detection of pigment changes during leaf senescence and fruit ripening. *Physiol. Plant.* **1999**, *106*, 135–141. [CrossRef]
182. Masiello, G.; Ripullone, F.; De Feis, I.; Rita, A.; Saulino, L.; Pasquariello, P.; Cersosimo, A.; Venafra, S.; Serio, C. The IASI Water Deficit Index to Monitor Vegetation Stress and Early Drying in Summer Heatwaves: An Application to Southern Italy. *Land* **2022**, *11*, 1366. [CrossRef]
183. Fuentes, S.; Tongson, E.; Viejo, C.G. Urban green infrastructure monitoring using remote sensing from integrated visible and thermal infrared cameras mounted on a moving vehicle. *Sensors* **2021**, *21*, 295. [CrossRef]
184. Zeng, Y.; Chen, M.; Hao, D.; Damm, A.; Badgley, G.; Rascher, U.; Johnson, J.E.; Dechant, B.; Siegmann, B.; Ryu, Y.; et al. Combining near-infrared radiance of vegetation and fluorescence spectroscopy to detect effects of abiotic changes and stresses. *Remote Sens. Environ.* **2022**, *270*, 112856. [CrossRef]

185. Cao, Y.X.; Huang, Z.; Xu, X.J.; Chen, S.; Wang, Z.; Feng, H.; Yu, Q.; He, J.Q. Responses of solar-induced chlorophyll fluorescence to meteorological drought across the Loess Plateau, China. *Chin. J. Appl. Ecol.* **2022**, *33*, 457–466. [CrossRef]
186. Dotzler, S.; Hill, J.; Buddenbaum, H.; Stoffels, J. The Potential of EnMAP and Sentinel-2 Data for Detecting Drought Stress Phenomena in Deciduous Forest Communities. *Remote Sens.* **2015**, *7*, 14227–14258. [CrossRef]
187. Moreno, A.; Maselli, F.; Chiesi, M.; Genesio, L.; Vaccari, F.; Seufert, G.; Gilabert, M.A. Monitoring water stress in Mediterranean semi-natural vegetation with satellite and meteorological data. *Int. J. Appl. Earth Obs. Geoinf.* **2014**, *26*, 246–255. [CrossRef]
188. Zhang, L.; Jiao, W.; Zhang, H.; Huang, C.; Tong, Q. Studying drought phenomena in the Continental United States in 2011 and 2012 using various drought indices. *Remote Sens. Environ.* **2017**, *190*, 96–106. [CrossRef]
189. Vacchiano, G.; Garbarino, M.; Mondino, E.B.; Motta, R. Evidences of drought stress as a predisposing factor to Scots pine decline in Valle d'Aosta (Italy). *Eur. J. For. Res.* **2012**, *131*, 989–1000. [CrossRef]
190. Chakraborty, T.; Sarkar, S.K.; Morshed, M.M. Big data and remote sensing for multi-decadal drought impact assessment on Shorea robusta. *Theor. Appl. Climatol.* **2022**, *148*, 1587–1602. [CrossRef]
191. Ciezkowski, W.; Szporak-Wasilewska, S.; Kleniewska, M.; Jozwiak, J.; Gnatowski, T.; Dabrowski, P.; Goraj, M.; Szatylowicz, J.; Ignar, S.; Chormanski, J. Remotely Sensed Land Surface Temperature-Based Water Stress Index for Wetland Habitats. *Remote Sens.* **2020**, *12*, 631. [CrossRef]
192. Drake, P.L.; Callow, N.J.; Leopold, M.; Pires, R.N.; Veneklaas, E.J. Thermal imagery of woodland tree canopies provides new insights into drought-induced tree mortality. *Sci. Total. Environ.* **2022**, *834*, 155395. [CrossRef]
193. Farhani, N.; Carreau, J.; Kassouk, Z.; Le Page, M.; Lili Chabaane, Z.; Boulet, G. Analysis of Multispectral Drought Indices in Central Tunisia. *Remote Sens.* **2022**, *14*, 1813. [CrossRef]
194. Springgay, E.; Ramirez, S.C.; Janzen, S.; Brito, V.V. The Forest–Water Nexus: An International Perspective. *Forests* **2019**, *10*, 915. [CrossRef]
195. Harper, R.; Smettem, K.R.J.; Ruprecht, J.K.; Dell, B.; Liu, N. Forest-water interactions in the changing environment of south-western Australia. *Ann. For. Sci.* **2019**, *76*, 95. [CrossRef]
196. Thammanu, S.; Marod, D.; Han, H.; Narayan Bhusal, L.A.; Ketdee, P.; Gaewsingha, N.; Lee, S. The influence of environmental factors on species composition and distribution in a community forest in Northern Thailand. *J. For. Res.* **2021**, *32*, 649–662. [CrossRef]
197. Wu, Z.; Yin, H.; He, H.; Li, Y. Dynamic-LSTM hybrid models to improve seasonal drought predictions over China. *J. Hydrol.* **2022**, *615*, 128706. [CrossRef]
198. Feng, P.; Wang, B.; Luo, J.-J.; Liu, D.L.; Waters, C.; Ji, F.; Ruan, H.; Xiao, D.; Shi, L.; Yu, Q. Using large-scale climate drivers to forecast meteorological drought condition in growing season across the Australian wheatbelt. *Sci. Total. Environ.* **2020**, *724*, 138162. [CrossRef]
199. Valeriano, C.; Gazol, A.; Colangelo, M.; González de Andrés, E.; Camarero, J.J. Modeling Climate Impacts on Tree Growth to Assess Tree Vulnerability to Drought During Forest Dieback. *Front. Plant Sci.* **2021**, *12*. Available online: https://www.frontiersin.org/articles/10.3389/fpls.2021.672855/full (accessed on 18 November 2022). [CrossRef]
200. Uddin, J.; Li, Y.; Sattar, A.; Mistry, S. Climatic water balance forecasting with machine learning and deep learning models over Bangladesh. *Int. J. Climatol.* **2022**, *42*, 10083–10106. [CrossRef]
201. Avetisyan, D.; Borisova, D.; Velizarova, E. Integrated Evaluation of Vegetation Drought Stress through Satellite Remote Sensing. *Forests* **2021**, *12*, 974. [CrossRef]